Article No. jmbi.1998.2348 available online at http://www.idealibrary.com on IDEAL J. Mol. Biol. (1999) 285, 755–773

JMB

Solution Structures of Micelle-bound Amyloid β-(1-40) and β-(1-42) Peptides of Alzheimer's Disease

Haiyan Shao, Shu-chuan Jao, Kan Ma and Michael G. Zagorski*

Department of Chemistry
Case Western Reserve
University, Cleveland
OH 44106, USA

The amyloid β-peptide is the major protein constituent of neuritic plaques in Alzheimer's disease. The β-peptide varies slightly in length and exists in two predominant forms: (1) the shorter, 40 residue β-(1-40), found mainly in cerebrovascular amyloid; and (2) the longer, 42 residue β-(1-42), which is the major component in amyloid plaque core deposits. We report here that the sodium dodecyl sulphate (SDS) micelle, a membrane-mimicking system for biophysical studies, prevents aggregation of the β-(1-40) and the β-(1-42) into the neurotoxic amyloid-like, β-pleated sheet structure, and instead encourages folding into predominantly α-helical structures at pH 7.2. Analysis of the nuclear Overhauser enhancement (NOE) and the αH NMR chemical shift data revealed no significant structural differences between the β-(1-40) and the β-(1-42). The NMR-derived, three-dimensional structure of the β-(1-42) consists of an extended chain (Asp1-Gly9), two α-helices (Tyr10-Val24 and Lys28-Ala42), and a looped region (Gly25-Ser26-Asn27). The most stable α-helical regions reside at Gln15-Val24 and Lys28-Val36. The majority of the amide (NH) temperature coefficients were less than 5, indicative of predominately strong NH backbone bonding. The lack of a persistent region with consistently low NH coefficients, together with the rapid NH exchange rates in deuterated water and spin-labeled studies, suggests that the β-peptide is located at the lipid-water interface of the micelle and does not become inbedded within the hydrophobic interior. This result has implications for the circulation of membrane-bound β-peptide in biological fluids, and may also facilitate the design of amyloid inhibitors to prevent an α-helix → β-sheet conversion in Alzheimer's disease.

*Corresponding author

Keywords: amyloid; β-peptide; NMR; micelle; Alzheimer's disease

Introduction

The brains of patients with Alzheimer's disease (AD) are characterized by an abundance of amyloid deposits (Iqbal *et al*., 1997; Smith, 1998). For amyloid of the cerebral vasculature, the major protein constituent is the 40 residue β-(1-40) peptide, while the predominant component in senile plaque cores in the parenchyma is the 42 residue β-(1-42). The β-peptides are derived from proteolytic processing of the much larger (695-770 amino acid residues) amyloid precursor proteins (APP), which are constitutively produced transmembrane glycoproteins that are expressed in a variety of cells during normal cellular metabolism (Selkoe, 1994).

Recent genetic evidence from early onset cases of AD established that amyloid formation by the β-(1-42) plays a key role in promoting the disease (Hardy, 1997). The genes responsible for the

Abbreviations used: AD, Alzheimer's disease; Apo-E, apolipoprotein-E; Apo-J, apolipoprotein-J; APP, amyloid precursor protein; CD, circular dichroism; CSI, chemical shift indices; EDTA, ethylenediamine tetraacetic acid; FT-IR, Fourier transform infra-red spectroscopy; HDL, high-density lipoproteins; HFIP, hexafluoroisopropanol; HPLC, high performance liquid chromatography; MS, mass spectrometry; NMR, nuclear magnetic resonance; NOESY, nuclear Overhauser enhancement spectroscopy; ^{1}H, proton; NaN_3, sodium azide; SDS, sodium dodecyl sulfate; TFA, trifluoroacetic acid; TFE, trifluoroethanol; TOCSY, total correlation spectroscopy; TSP, sodium 3-(trimethylsilyl)propionate-2,2,3,3-d_4; 2D, two-dimensional; 1D, one-dimensional; 3D, three-dimensional.

E-mail address of the corresponding author: mxz12@po.cwru.edu

0022-2836/99/020755–19 $30.00/0

inherited cases have mutations in the APP, and another group of homologous proteins called the presenilins (Levy-Lahad *et al.*, 1995), all of which result in selective processing of APP to produce preferentially the β-(1-42) rather than the β-(1-40). These results, together with other biophysical studies demonstrating that the β-(1-42) can nucleate amyloid formation of the more soluble protein β-(1-40; Harper & Lansbury, 1997), indicates that the β-(1-42) may be the actual culprit for initiating amyloid deposition in AD (Younkin, 1995).

Considerable experimental data alleges that there is a direct association between the accumulation of β-peptide into amyloid and the severity of dementia in AD. In the brain, the β-peptide can fold into soluble, monomeric random coil and α-helical structures, as well as the less soluble, aggregated (oligomeric) β-sheet structure (Choo *et al.*, 1996). The β-sheet is mostly fibrillar and is the predominant motif in the amyloid plaque core (Kirschner *et al.*, 1986; Malinchik *et al.*, 1998). In earlier diffuse or preamyloid deposits, the β-peptide is non-fibrillar and presumably folds into mixtures of random coil, α-helix, and β-sheet structures. It is now generally accepted that during these β-aggregation processes, the β-peptide undergoes a conformational rearrangement (α-helix → β-sheet and/or random coil → β-sheet) that promotes toxicity to nerve cells (Simmons *et al.*, 1994; Pike *et al.*, 1995). Once deposited as dense amyloid plaque cores, the surrounding nerve cells are dystrophic and the β-peptide becomes highly resistant to further proteolysis (Knauer *et al.*, 1992; Nordstedt *et al.*, 1994; Wisniewski *et al.*, 1994). As a result, major research efforts are focused on uncovering workable therapeutic strategies to prevent these conformational conversions, which in turn will curtail the neurotoxicity and amyloid plaque formation in AD.

The importance of β-peptide/lipid interactions in AD is well documented. In virtually all biological fluids, the β-peptide binds to various hydrophobic macromolecules such as apolipoproteins (Apo-E and Apo-J), high-density lipoproteins (HDL), albumin, transthyretin, proteasomes, α_2-macroglobulin, and other lipoproteins, which may have relevance for the circulation of the β-peptide (Schwarzman *et al.*, 1994; Roses, 1995; Biere *et al.*, 1996; Koudinov *et al.*, 1996; Matsubara *et al.*, 1996; Du *et al.*, 1998). Other research has shown that interactions of the β-peptides with lipid bilayers or neuronal membranes can increase the fluidity and intracellular calcium levels, produce voltage-dependent ion channels, and exert other effects such as blockage and excitability on potassium channels (Arispe *et al.*, 1993; Mattson *et al.*, 1993; Good & Murphy, 1996; Avdulov *et al.*, 1997; Kawahara *et al.*, 1997). These latter processes, along with the aggregation into β-sheet structures, are thought to be involved in the β-peptide-induced neurotoxicity. Taken together, these results demonstrate that the aggregation state and structure of the β-peptide in membrane-like environments are important pathological events in AD.

To provide a molecular basis for the role of biological membranes in amyloid formation, the solution structures of the β-(1-40) and β-(1-42) peptides in detergent micelles was investigated using NMR spectroscopy. The approach of using micelles such as the negatively charged sodium dodecyl sulphate (SDS) to mimic the molecular environment of biological membranes has been successfully applied to many peptides and proteins (McDonnell & Opella, 1993; Henry & Sykes, 1994). Our results establish that the α-helix is the predominate structural motif in SDS solution and that the β-peptides associate at the micelle surface, rather than within the hydrophobic core. The implications of these findings to amyloid formation and to the circulation of the β-peptide in biological fluids are discussed.

Results

Preliminary considerations

Biophysical studies of the synthetic β-peptides, especially the β-(1-42), are plagued by many difficulties (Teplow, 1998). The biggest problem relates to their time-dependent aggregation in aqueous solution, which is serious for NMR experiments since higher concentrations (several mM) are generally required. During the aggregation, the more soluble random coil and α-helix structures rearrange into the less soluble oligomeric β-sheet, which eventually precipitates as an amyloid-like deposit. This dilemma has clearly precluded NMR studies of the naturally occurring β-(1-40) and β-(1-42) peptides in water solution.

To overcome these difficulties, we performed two modifications in the sample preparation procedure. First, we used a simple TFA pre-treatment protocol (Jao *et al.*, 1997), which addressed problems related to the different starting aggregation states and structures of the β-peptides (Soto *et al.*, 1995b). The second modification in the sample preparation procedure addressed the β-peptide time-dependent aggregation. Here, we fortuitously discovered that the SDS micelle not only provided an appropriate membrane-mimicking system for NMR, but also prevented aggregation of the β-(1-40) and β-(1-42) peptides, analogous to what we had observed with the shorter β-(1-28) (Talafous *et al.*, 1994; Marcinowski *et al.*, 1998). In fact, the more aggregation prone, β-(1-42) is stable at relatively high concentrations (up to 2 mM) in aqueous SDS solutions for several months. The stability and lack of precipitation of the β-(1-42) indicated that the SDS micelle provides an amenable environment for detailed structural analysis by high-resolution NMR methods. This ability of SDS to prevent aggregation is analogous to other recent work, where other charged micelles, such as hexadecyl-*N*-methylpiperidinium bromide, inhib-

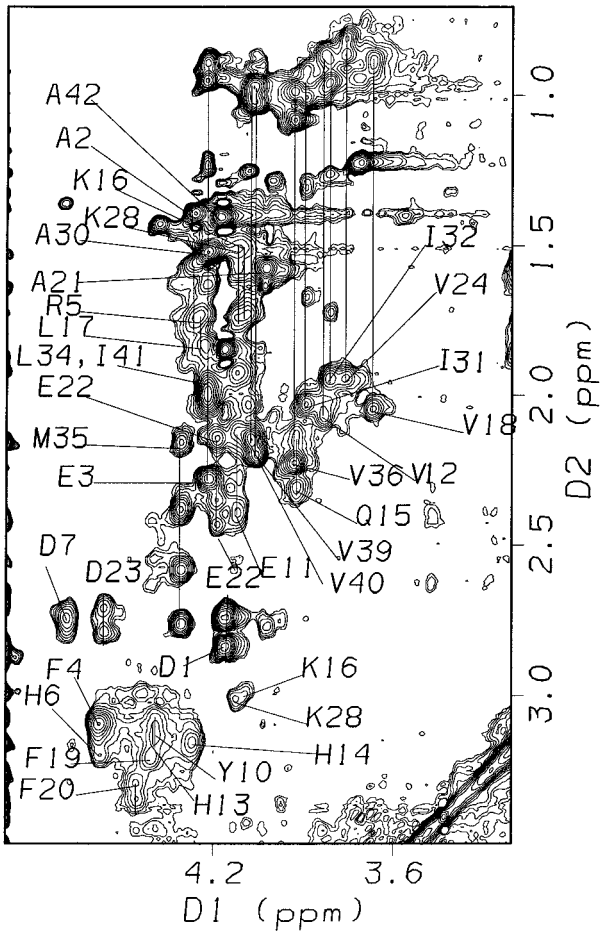

Figure 1. Expanded aliphatic region of a clean-TOCSY (MLEV-17 spin lock time 70 ms) for the 1.4 mM β-(1-42) in H_2O:^2H_2O (9:1) containing 115 mM SDS-d_{25} at pH 7.2 and 20 °C. Many direct (two and three-bond) and relay (greater than three-bond) assignments are shown. The four resolved peaks for the $C^{\beta}H_3$-H^{α} couplings of Ala2, Ala21, Ala30 and Ala42 (upper section) establish that the major solution conformation is folded. Other useful couplings are the long-range $C^{\alpha}H$ to $C^{\varepsilon}H_2$ relayed connectivities, which were particularly helpful for uncovering the Lys H^{α} among those for the Leu and Ile.

ited aggregation of the β-(1-40) (Wood *et al.*, 1996b).

Before beginning with extensive two-dimensional (2D) NMR work, using circular dichroism (CD) and one-dimensional (1D) NMR we first examined the effect of salts, and varied peptide and SDS concentrations on the secondary structure of the β-(1-42). To produce uniform micelles at low ionic strength, 62 monomers of SDS (average aggregation number) are required at concentrations above 8 mM (critical micelle concentration; Henry & Sykes, 1994). With the exception of minor chemical shift differences for some residues at the N terminus, 1D NMR spectra at β-(1-42) concentrations of 1.4, 0.94, 0.56, and 0.16 mM were virtually identical in the aliphatic and aromatic regions. These data establish that the β-peptides are monomeric in water-SDS solution, consistent with results from CD (H.S. & M.G.Z., unpublished results). Here, all 2D NMR measurements were done at elevated SDS concentrations, well above the critical micelle concentration and at high micelle:peptide ratios (McDonnell & Opella, 1993). The sample stability was checked by comparing 1D spectra before and after the 2D acquisitions that usually required 10-20 hours of data accumulation.

The CD studies in SDS solution at pH 7.2 with and without salt (30-150 mM sodium fluoride) were approximately identical and consistent with predominantly α-helical structure. This indicates that the ionic strength is not a critical parameter for the micelle-induced secondary structure of the β-(1-42). These results are compatible with previous studies where salts such as NaCl had little effect on the binding of the β-(1-40) to rat cortical homogenates (lipids and membrane-associated proteins) and to artificial neuronal membranes (lipids only; Good & Murphy, 1995).

Spin system identification, sequential assignments, and secondary structural analysis

The 2D nuclear Overhauser enhancement spectroscopy (NOESY) spectra of the β-(1-40) and β-(1-42) in SDS-H_2O solution at pH 7.2 displayed numerous, well-resolved cross-peaks, indicating that the peptides are folded and that assignments should be possible using standard homonuclear NMR methods (Wüthrich, 1986; Case & Wright, 1993). For example, as shown in the expanded total correlation spectroscopy (TOCSY) spectrum (Figure 1), there are distinct chemical shifts for the six Val (Val12, Val18, Val24, Val36, Val39, Val40) and the four Ala (Ala2, Ala21, Ala30, Ala42) residue, whereas if the peptide were unfolded or random coil, then the six βCH and the four βCH_3 signals of the Val and Ala residues would be nearly degenerate. Shown in Figure 2 is an expanded NH-NH region of the NOESY spectrum for the β-(1-42). This spectrum demonstrates numerous NOEs such as the NN(i, $i+1$), diagnostic for α-helices, and additional inter and intraresidue NOEs from the aromatic ring protons of Tyr10, Phe19, and Phe20 to nearby backbone NH protons.

Most of the spectral overlap occurred in the αH-NH region (3.5-5.5 and 7.2-9 ppm), which was overcome by comparing data at different temperatures. Spectra obtained at mixing times of 120 and 270 ms were nearly identical, except that as expected, the longer mixing time produced somewhat stronger cross-peaks. The few additional weak NOEs present in the longer mixing time NOESY, such as those between the aromatic sidechains and neighboring backbone amide (NH) signals, were not used as constraints in the tertiary structure analysis. The complete ^1H NMR assignments for the β-(1-40) and β-(1-42) are summarized in the Supplementary Material, and a complete

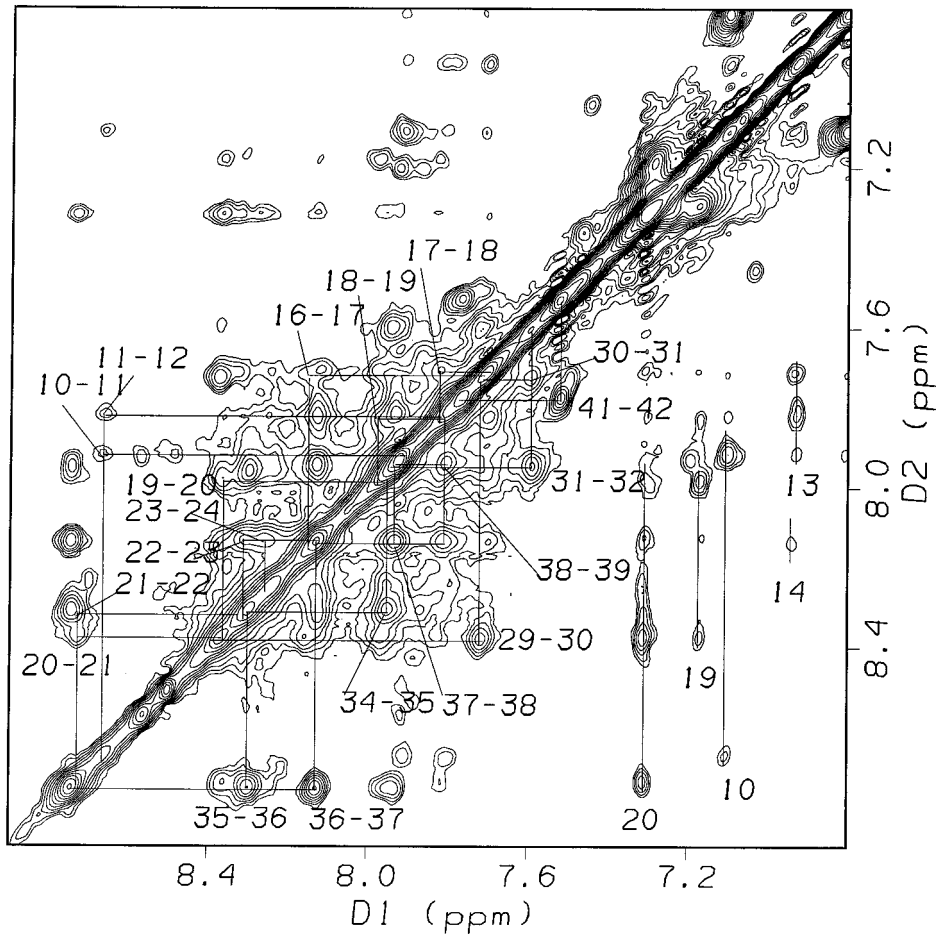

Figure 2. Expanded NOESY region for the β-(1-42) showing the NH-NH connectivities as well as other NOE interactions between the aromatic side-chains and the backbone-NH. The NH assignments for the two principal α-helical regions (Tyr10-Val24 and Lys28-Val36) are depicted on opposite sides of the diagonal.

Figure 3. Summary of the inter-residue NOEs among the backbone NH, αH, and βH for the β-(1-42). The NOE intensities are reflected by the thickness of the lines. When an unambiguous assignment was not possible due to peak overlap, the NOEs are drawn with gray shaded boxes.

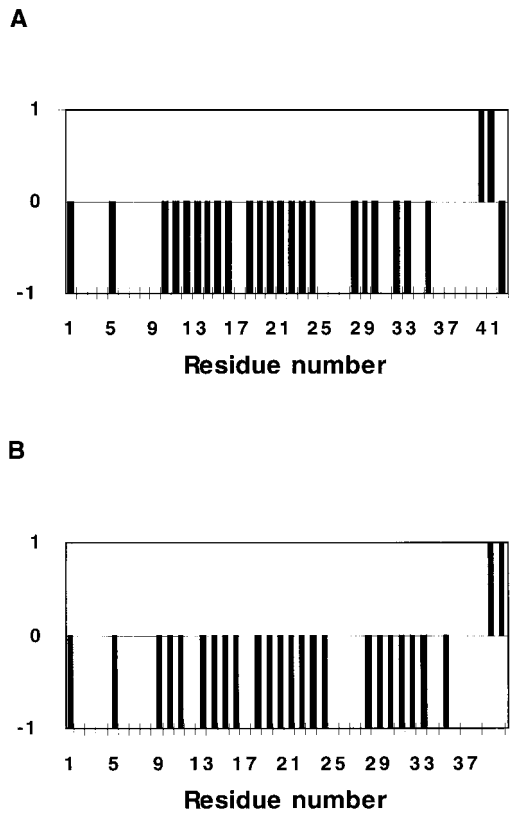

Figure 4. The αH chemical shift indices for the β-(1-40) and β-(1-42) in SDS solution at pH 7.2. The indices are −1, 0 or 1, which corresponds with either α-helix, random coil, or β-sheet (Wishart *et al.*, 1992). These data demonstrate that both peptides are primarily α-helical, particularly within the Tyr10-Val24 and Lys28-Val36 regions.

summary of the inter-residue NOE connectivities for the β-(1-42) is shown in Figure 3.

As shown in Figures 2 and 3, the NN(i, $i+1$) NOEs for the β-(1-42) reside in two main peptide segments: Tyr10-Val24 and Lys28-Ala42. There is also a contiguous stretch of medium-range, αβ(i, $i+3$) NOEs within the Tyr10-Val24 region, while the αN(i, $i+3$) and αN(i, $i+4$) NOEs are localized at Leu17-Ala21. These data support the presence of a predominantly α-helical structure within the Tyr10-Val24 region, with the central Leu17-Ala21 acting as a more stable core. The Lys28-Ala42 region has similar sequential and backbone NOE patterns, except that three αβ(i, $i+3$) NOEs are absent, due to the lack of βHs for Gly33, Gly37, and Gly38. The absence of any αN(i, $i+2$) NOEs and the presence of several αN(i, $i+4$) NOEs at Leu17-Val24 and Gly29-Val39 rule out the possibility of 3_{10}-helices that could be equilibrating with the α-helices. Analysis of the β-(1-40) and β-(1-42) using αH chemical shift indices (CSI) showed that they are mostly upfield and compatible with a disordered structure at Gly25-Ser26-Asn27, and α-helices at Tyr10-Val24 and Lys28-Val36 (Wishart *et al.*, 1992; Figure 4). Taken together, the NOE and CSI data support the presence of α-helices at Tyr10-Val24 and Lys28-Ala42, with the Asp1-Gly9 region being mostly extended chain and the Gly25-Ser26-Asn27 acting as a connecting loop between the two α-helices.

The NOE and αH CSI data for the β-(1-40) and β-(1-42) are more or less indistinguishable, thus demonstrating that both peptides adopt identical backbone secondary structures in SDS solution, in accordance with their nearly identical NOE data. Interestingly, the Val39-Val40 and Val40-Ile41 regions for the β-(1-40) and β-(1-42) have downfield αH shifts, indicating some propensity for β-sheet structure. These shifts may be the result of conformational averaging between the predominantly α-helix (micelle-bound species) and β-sheet that forms when the peptides leave the micelle surfaces. It is well known that the last C-terminal residues play critical roles in initiating β-sheet formation and amyloid deposition in AD (Harper & Lansbury, 1997).

Final analysis of the secondary structure was explored using the NH chemical shifts, which can be directly correlated with hydrogen bond strengths and α-helix bending. For bent amphipathic α-helices, the NH typically display a periodic 3-4 repeat periodicity in chemical shifts, where the convex and concave sides of the α-helix promote upfield and downfield NH shifts, respectively (Kuntz *et al.*, 1991; Zhou *et al.*, 1992). Shown in Figure 5 is a plot of the differences between the NH observed chemical shifts of the β-(1-42) and those expected for each amino acid residue in a random coil conformation (Wishart *et al.*, 1995). This subtraction procedure removed any residue-specific effects. The majority of the NH signals for the β-(1-42) are shifted upfield relative to random coil values, indicative of α-helical structure. The 3-4 repeat pattern for the Phe19-Val24 and Lys28-Val36 regions, together with the low field NH shifts for Ala21, Val24, and Val36 (indicative of shorter H−O bond distances), establish that some curvature of the α-helices may be present. In contrast, the lack of chemical shift periodicity of the Gln15-Phe19 and Gly37-Ile41 regions suggests an absence of any significant α-helical bending in these regions.

Hydrogen exchange experiments

The location of the β-(1-42) peptide relative to the SDS micelle, as well as the solvent accessibility of the NH signals, was explored by proton-deuterium exchange studies. These measurements involved dissolving a protonated β-(1-42) sample containing SDS-d_{25} in ^2H_2O and subsequently monitoring the disappearance of the NH peaks by 1D and 2D NMR. Analysis of the 1D spectra after 30 minutes showed that nearly all of the NH signals had disappeared. The few, remaining weak signals correspond to Ala21, Val36, and other residues with NH signals at 7.8-8.0 ppm. These weak

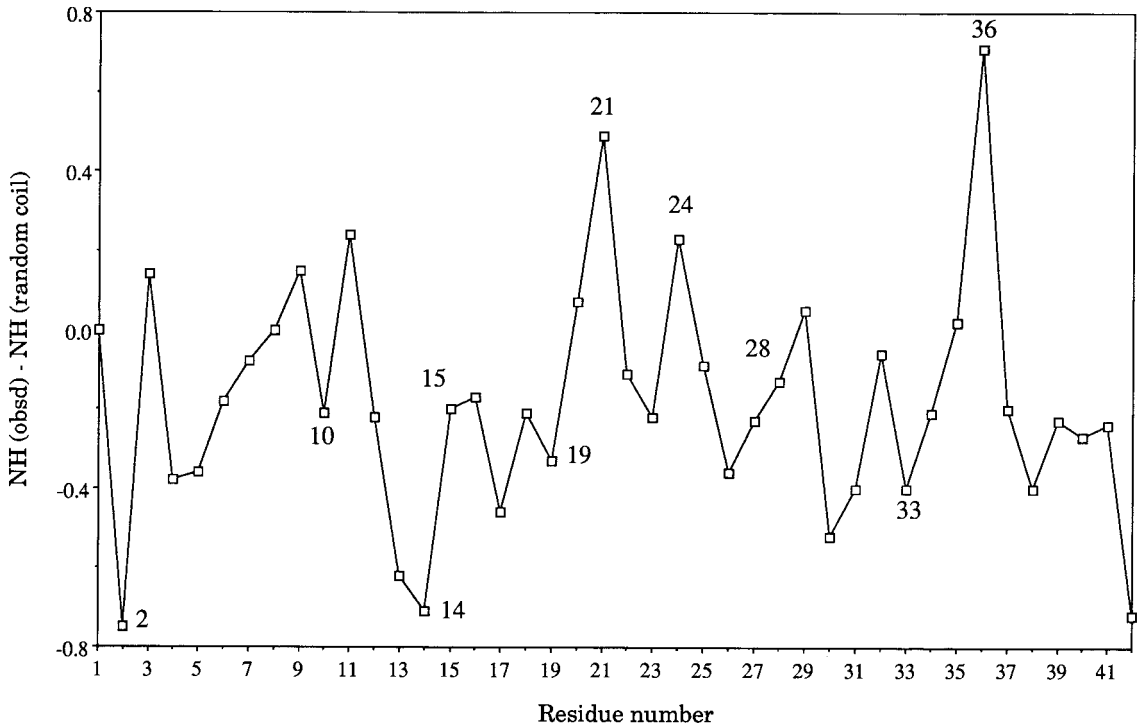

Figure 5. Graph showing the differences between the NH chemical shifts for the β-(1-42) in SDS at pH 7.2 and those expected for each amino acid residue in a random coil conformation (Wishart *et al.*, 1995). The primary sequence is shown on the ordinate and the assignments for some NH resonances are further highlighted in the graph.

signals could not be unambiguously assigned to specific residues, since they disappeared during the two to four hour period that was used to acquire the 2D NOESY data.

Temperature dependence of NH chemical shifts

For the β-(1-42), the temperature dependence of the NH chemical shifts was determined. This information provides a temperature coefficient, which is an extremely useful parameter for defining relative hydrogen bond strengths and solvent accessibility of labile protons (Dyson *et al.*, 1988).

The NH chemical shifts were obtained from NOESY spectra within a 15-30 °C range, since the NOE intensities became weak outside these limits (Figure 6). The loss of NOEs at higher temperatures may result of some α-helix unfolding, while below 15 °C the solution became viscous causing the NH signals to broaden. Because of problems with spectral overlap or rapid exchange rates, NH coefficients could not be determined for Asp1, Ala2, or Lys16. Most of the NH signals displayed the typical upfield shifts with increasing temperature, although the NH protons for Gly9, Glu11, Gln15, Asp23, Ser26, and Ala30 showed downfield shifts with increasing temperature, resulting in negative coefficients. These downfield shifts may be due to greater solvent protection of some NH protons or possibly localized α-helix unfolding at the higher temperatures.

Altogether, as depicted graphically in Figure 6, the NH coefficients varied between −0.8 and 8.2, with most residues exhibiting little chemical shift variation with temperature, producing coefficients less than 5, typical of strong NH bonding. The NH coefficients greater than or equal to 5 were from Arg5, Ser8, His13, Phe19, Phe20, Val24, and Val36, indicative of weaker NH bonding. Both Phe19 and Phe20 have large coefficients with the β-(1-28) peptide when folded as an α-helix in TFE-water and SDS-water solutions (Zagorski & Barrow, 1992; Marcinowski *et al.*, 1998). These data, together with the somewhat high Val18 coefficient of 4.4, suggests that the Val18-Phe19-Phe20 α-helix segment is the first to unfold at elevated temperatures for both the β-(1-28) and β-(1-42) peptides. The importance of the Val18-Phe19-Phe20 region for induction of β-amyloidosis is well documented (Hilbich *et al.*, 1992; Wood *et al.*, 1995; Esler *et al.*, 1996a). For example, a β-(1-40) peptide with a Val18 → Ala mutation showed increased α-helix stability and was less likely to form β-sheet fibrils by an α-helix → β-sheet rearrangement (Soto *et al.*, 1995a).

Spin-labeled studies

To further explore the possibility of β-peptide insertion into the hydrophobic micelle core, we undertook NMR studies using the spin-labeled 12-doxylstearic acid. This compound contains a spin label that is covalently attached to position 12,

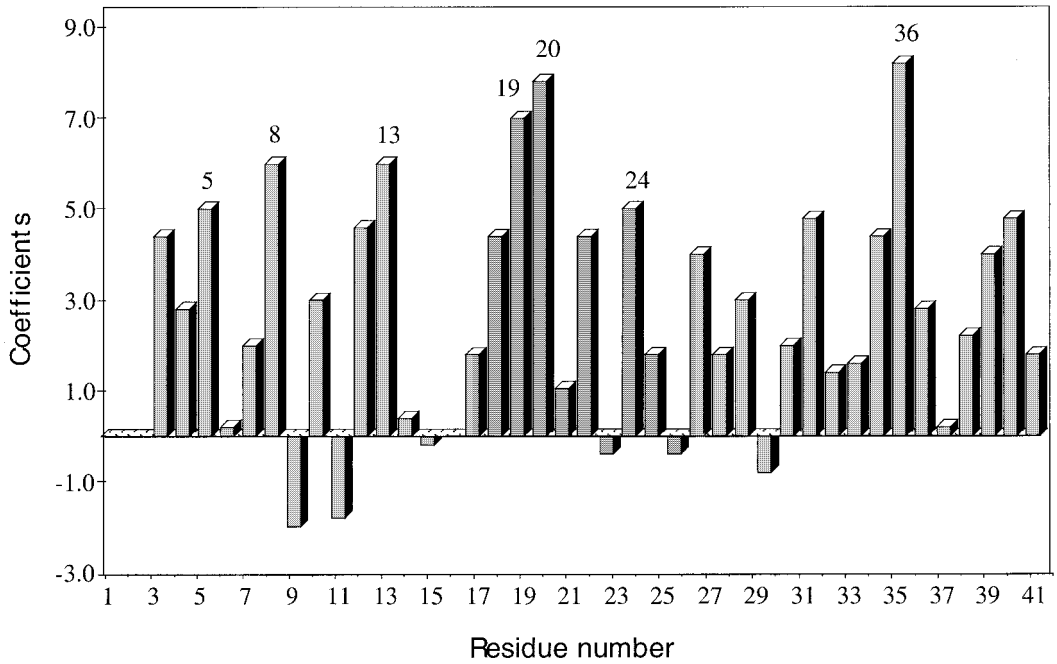

Figure 6. Amide-NH temperature coefficients for the β-(1-42), which were taken from the slopes of the least-square computer fitted lines of the chemical shifts against temperature. The data were obtained from NOESY spectra at 15-30 °C.

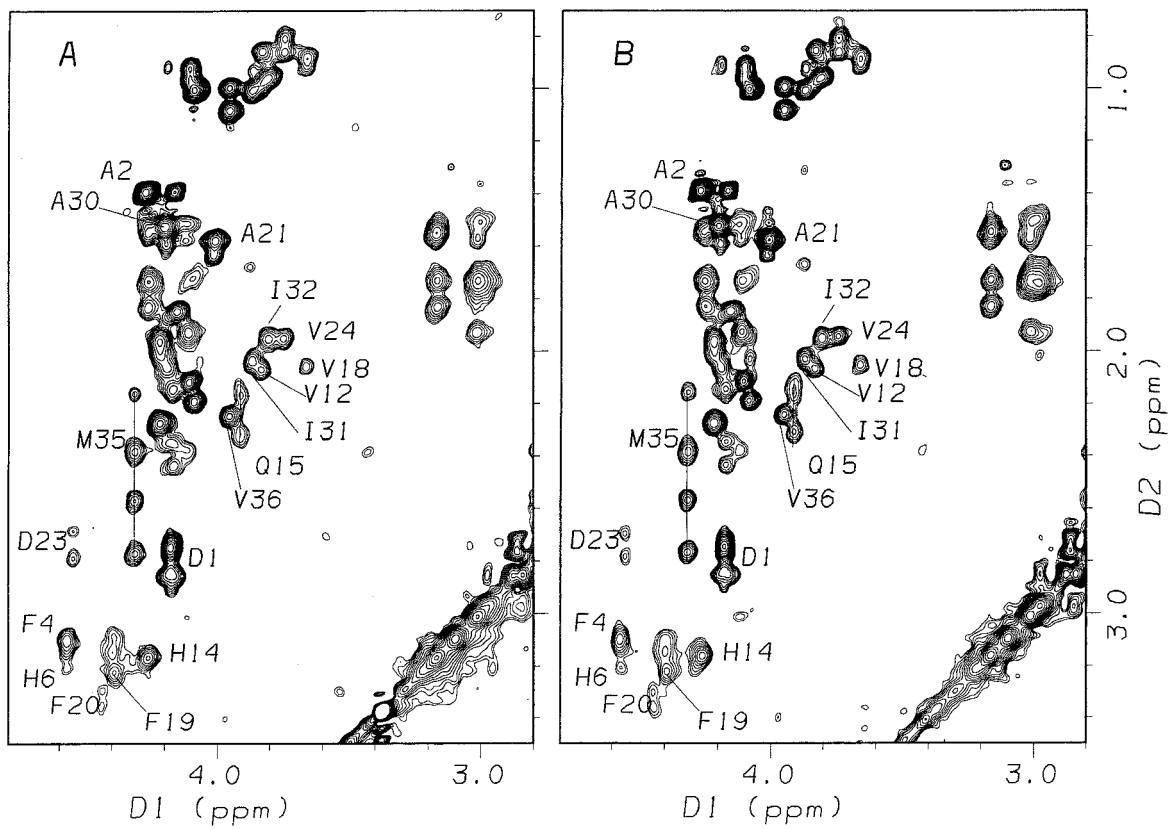

Figure 7. Expanded aliphatic region of TOCSY spectra for β-(1-40) in SDS solution with (a) and without (b) the presence of the spin-labeled 12-doxylstearic acid.

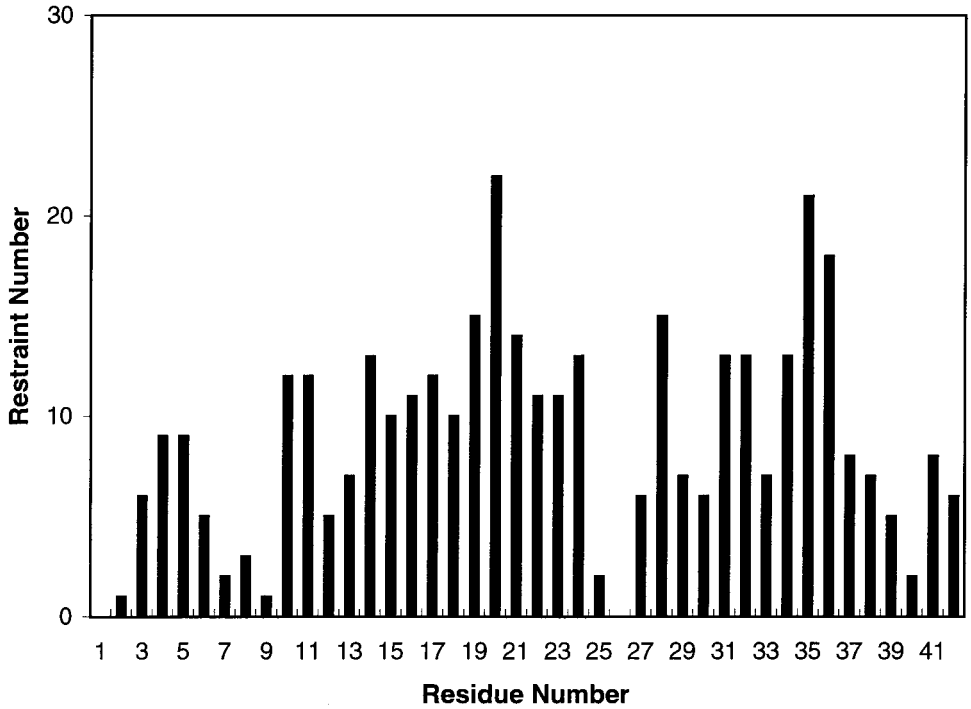

Figure 8. Survey of the NOE distance restraints *versus* the β-(1-42) amino acid sequence. The restraints includes both intra- and inter-residue NOE data.

Table 1. Statistical information for the β-(1-42) structure calculation

Distance restraints	Total	246
	Intra-monomer	121
	Inter-monomer	125
	Sequential ($i - j = 1$)	84
	Medium ($i - j = 2, 3, 4$)	41
RMSD[a] analysis (Å)	Gln15-Val24 backbone[b]	0.87 ± 0.34
	Gln15-Val24 heavy atoms[c]	0.87 ± 0.34
	Lys28-Val36 backbone	1.27 ± 0.41
	Lys28-Val36 heavy atoms	1.21 ± 0.39
Structure check[d] (%)	Gln15-Val24: Average	54.2
	Highest	93.3
	Lowest	40
	Lys28-Val36: Average	52
	Highest	78.6
	Lowest	35.7
NOE violations > 0.2 Å	Total violations	8
	Highest	0.35
	Lowest	0
	Average violation (Å)	0.28 ± 0.05
Average energy (kcal/mol)	Total energy	398 ± 86
	Bond energy	127 ± 3
	Phi energy	72 ± 9
	Theta energy	258 ± 10
	Out of plane energy	4 ± 1
	Non-bonded energy	240 ± 19
	Coulomb energy	-303 ± 89

[a] Atomic root mean square deviation calculated by superimposing the corresponding region of the 15 minimized structures referenced by the mean coordinates.
[b] Includes the C^{α}, N, C atoms.
[c] Includes the C, N, O atoms.
[d] The percentages represent the ϕ and φ angles falling within the allowed Ramachandran regions for the best-fit 15 minimized structures.

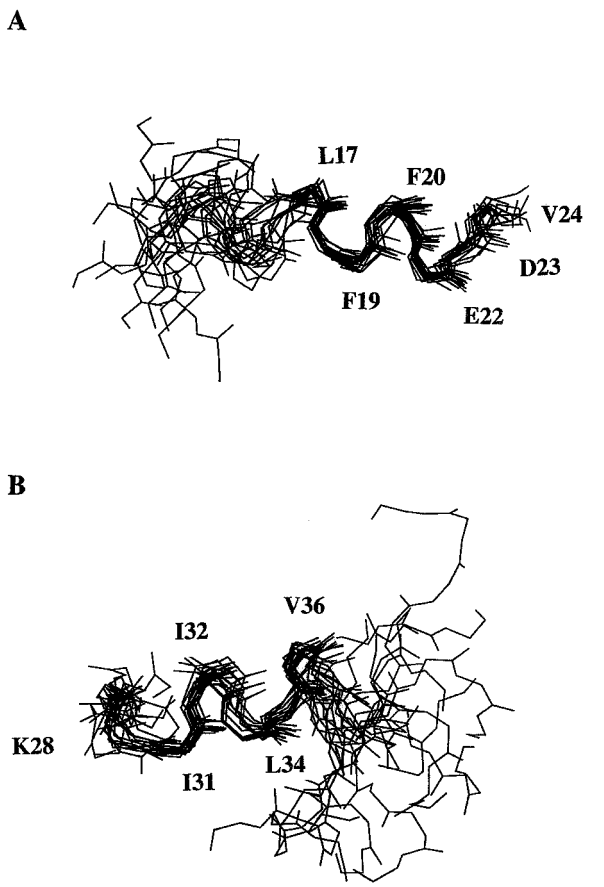

Figure 9. The superposition of 15 minimized structures for the β-(1-42) using the backbone atoms (C^{α}, N and C). (a) Tyr10-Gly25 by superimposing residues Gln15-Val24; (b) Lys28-Ala42 by superimposing Lys28-Val36.

thereby providing a free radical in the center of micelle (Papavoine *et al*., 1994; Chupin *et al*., 1995). Consequently, peptide residues that are likewise buried in the micelle center will become selectively broadened in the presence of 12-doxylstearic acid.

Shown in Figure 7 are TOCSY spectra for a β-(1-40)-SDS solution taken before and after the addition of 12-doxylstearic acid. The molar ratios were sufficient to ensure that there was one molecule of peptide and relaxation reagent per SDS micelle. As shown, the intensities of the TOCSY cross-peaks are virtually indistinguishable between the two spectra, which is consistent with the absence of β-peptide residues within the micelle core.

Three-dimensional structures

Because the NMR-derived secondary structures for the β-(1-40) and β-(1-42) were essentially identical, tertiary structure calculations were performed for only the longer β-(1-42). As discussed before, the β-(1-42) is more physiologically relevant and is linked to many early onset forms of AD.

A total of 246 NOE-based distance restraints were used in the structure calculations, with the majority of the restraints located at the two presumed α-helical regions (Tyr10-Val24 and Lys28-Ala42; Figure 8). Due to the lack of restraints in the other regions, the overall convergence of the final structures was somewhat low when spread over the entire molecule. Significant structural variation was present in the Asp1-Gly9 and Gly25-Ser26-Asn27 regions, which is consistent with the absence of sufficient NOE data (Figure 8). Since these areas are presumably extended chain and conformationally mobile, they were not further analyzed. To explore the structure and dynamics at these sites, additional NMR relaxation time measurements are currently being performed and will be reported in a forthcoming paper.

For the present study we focused our attention to the Tyr10-Val24 and Lys28-Ala42 regions that had better structural convergence, with atomic root mean square deviations (RMSD) for backbone atoms of 1.40(±0.60) and 1.82(±0.68), respectively. From the 18 minimized structures, 15 structures with distance violations less than 0.35 Å were selected for further analysis. A residue-specific RMSD and other parameters (Table 1) established relatively good agreement among the final computed structures. Both the Tyr10-Val24 and Lys28-Ala42 regions were largely α-helical, as highlighted with the overlaid structures in Figure 9. The α-helices at Gln15-Val24 and Lys28-Val36 are the best defined (RMSD of 0.9 and 1.2), whereas the Tyr10-His14 and Gly37-Ala42 regions are less structured and have higher pairwise RMSD. These results agree with the conclusions made on the basis of the NOE and chemical shift data, i.e. the less defined Gly37-Ala42 α-helix results from the absence of several medium-range NOEs and the flexible Gly37-Gly38 segment.

A notable feature of the tertiary structure is that the two α-helices are somewhat proximate and antiparallel. This antiparallel alignment is energetically favorable, since it allows the two α-helical dipoles to run in opposite directions (Shoemaker *et al*., 1987). For the best 15 structures, the average distances between the α-carbons of Val24 ↔ Lys28 and Tyr10 ↔ Ala42 was 9.2(±1.2) Å and 28.9(±10.7) Å, respectively. As expected, long-range NOE interactions between the two α-helices were not observed, which is probably due to the flexible Gly25-Ser26-Asn27 loop segment that causes the side-chains atoms to be greater than 5 Å apart.

Discussion

Conformity of the tertiary structure with the NMR data and comparison with previous studies

The three-dimensional structure of the β-(1-42) agrees well with the NMR data. Overall, the structure consists of an extended strand (Asp1-Gly9),

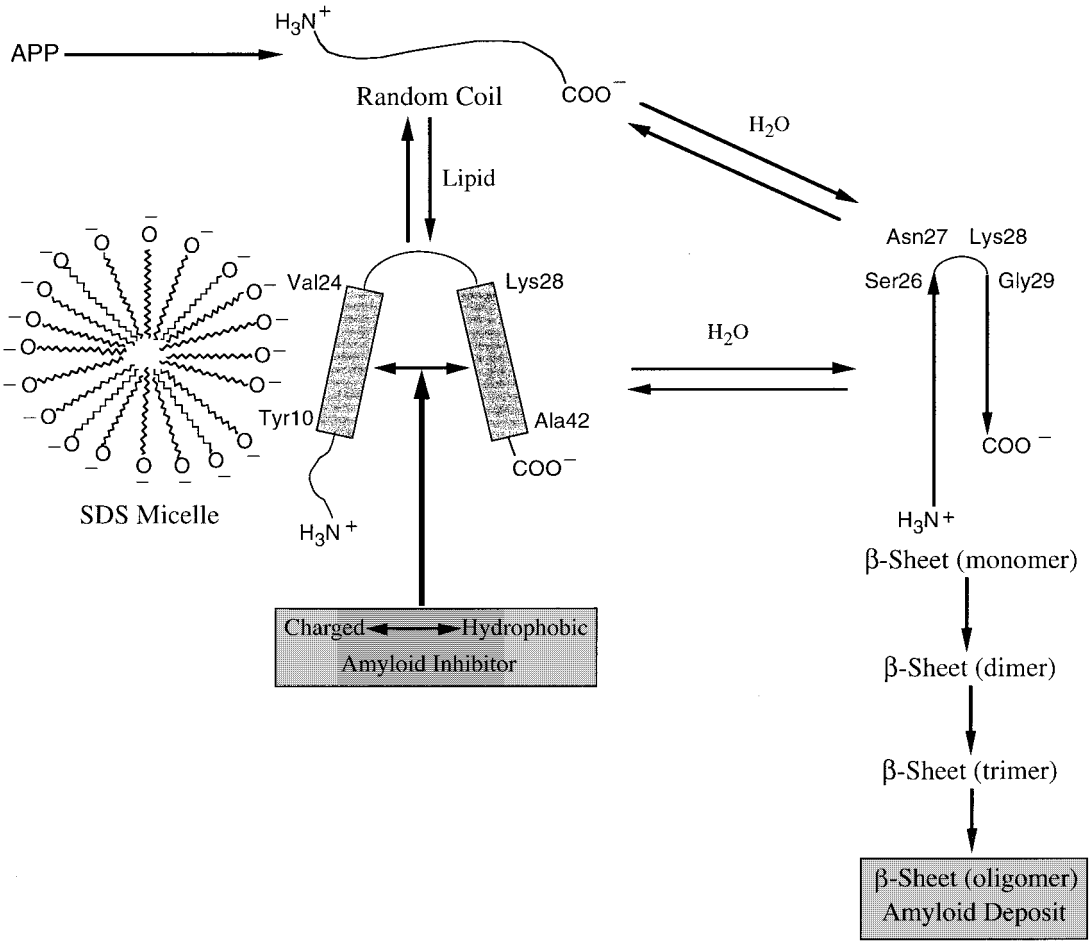

Figure 10. Proposed mechanism of β-amyloidosis for the β-(1-42), that involves formation of a largely α-helical structure when bound to the SDS micelle or a similar negatively charged biological lipid. The SDS micelle and peptide strands are not drawn according to their relative sizes. The α-helices are depicted with darkened cylinders, while the random coil or extended strand regions are drawn with wavy lines. The two α-helices (Tyr10-Val24 and Lys28-Ala42) are drawn in an antiparallel orientation on the basis of the structural data (see the text). The proposed monomeric β-sheet structure is based on previous studies showing a reverse turn at Ser26-Asn27-Lys28-Gly29 (Hilbich *et al.*, 1991), and recent NMR data from our laboratories for the β-(1-40) and β-(1-42) in water solution (H.S. & M.G.Z., unpublished results). In the brain, after proteolytic cleavage of APP, the β-(1-42) presumably adopts unfolded, random coil structure, which becomes mostly α-helical when bound to a negatively charged biological lipid. Aggregation to the β-sheet occurs from a brain micro-environmental changes such as localized regions of high peptide concentration or possibly small amounts of preformed β-sheet ("seed") material. The α-helical structure remains on the SDS or lipid surface and does not become imbedded into the hydrophobic interior. A potential amyloid inhibitor could be designed with polar and hydrophobic ends for docking between the charged (Tyr10-Val24) and hydrophobic (Lys28-Ala42) α-helices.

α-helix (Tyr10-Val24), loop (Gly25-Asn27), and α-helix (Lys28-Ala42). The numerous medium-range $\alpha\beta(i, i+3)$, $\alpha N(i, i+3)$ and $\alpha N(i, i+4)$ NOEs and the upfield shifted αH signals are consistent with α-helices at Tyr10-Val24 and Lys28-Ala42. The most stable and well-defined α-helices reside at Gln15-Val24 and Lys28-Val36, compatible with stable, three and two helical turns. The remaining Tyr10-His14 and Gly37-Ala42 regions are slightly disordered and may exist as an ensemble of α-helix and unfolded structures. The Gly25-Ser26-Asn27 residues act as a loop between the two α-helices, which is mobile as shown by the absence of any major backbone NOEs and the downfield chemical shift of the Asn27 αH. In fact, the majority of three residue loops between α-helices have Gly at the first position (Geetha & Munson, 1997). Interestingly, the location of this loop is nearly identical with the proposed Ser26-Asn27-Lys28-Gly29 reverse turn for the β-sheet structure of the amyloid β-(10-43) peptide fragment (Hilbich *et al.*, 1991).

Analysis of the NOE and the αH NMR chemical shift data revealed no significant structural differences between the β-(1-40) and the β-(1-42). This structural similarity suggests that the greater propensity of the β-(1-42) to aggregate as amyloid is not related to the membrane-bound structure.

Numerous biophysical studies using CD and Fourier transform infra-red spectroscopy (FT-IR)

have already explored β-peptide membrane interactions. A few discrepancies exist among these studies, which can partly be explained by differences in the membrane systems employed (i.e. charged, acidic, or neutral lipids), and by differences in the initial aggregation states and structures of the β-peptides (Soto *et al*., 1995b; Jao *et al*., 1997). Some studies showed that the β-sheet is a predominate structural motif on the membrane surface, which may or may not become partly imbedded into the membrane. As mentioned before, the β-sheet structure is neurotoxic, aggregated, and eventually precipitates as an amyloid plaque (Simmons *et al*., 1994; Pike *et al*., 1995). It was also found that some lipids (Klunk *et al*., 1997), including micelles (Wood *et al*., 1996b) and neutral lipid vesicles, promote random coil structure for the β-(1-40) peptide at physiological pH (Terzi *et al*., 1995). In contrast, mixtures of neutral and negatively charged lipid vesicles encourage α-helical structure at high lipid/peptide ratios (Terzi *et al*., 1997). For the latter study, it was also established that the α-helical structure for the β-(1-40) does not penetrate into hydrophobic vesicle interior, which is consistent with the present findings in micelle solution. However, our results disagree with an earlier report, in which according to CD the β-(1-42) peptide produced β-sheet structure in water-SDS solution (Otvos *et al*., 1993). One possibility is that, for the latter study, the β-(1-42) samples were already slightly pre-aggregated before performing the CD experiments, which would account for presence of mostly β-sheet structure. For the present study, these problems were alleviated for the more aggregation prone β-(1-42) by using our TFA pretreatment protocol (see Materials and Methods).

Due to problems with aggregation, only a limited number of solution NMR studies have been reported with the β-peptides. A recent concurrent NMR study of the β-(1-40) in SDS solution indicated that stable α-helices are present at Gln15-Val36 with a hinge region at Gly25-Asn27 (Coles *et al*., 1998), consistent with the present results. In regard to the other studies, it is important to recognize that often different solvent conditions and different sized peptides were employed, so the structures often show some variations. The NMR-derived tertiary structure for the β-(1-40) peptide in 40% (v/v) trifluoroethanol (TFE) solution reportedly contained two well-defined α-helices at Gln15-Asp23 and Ile31-Met35 (Sticht *et al*., 1995). In contrast, the NMR-derived three-dimensional (2D) structure for the β-(25-35) peptide was completely α-helical in SDS solution, with the N-terminal region exposed to solvent and the C-terminal region located in the hydrophobic interior (Kohno *et al*., 1996), which supports other studies of the β-(25-35) in bilayer membranes (Mason *et al*., 1996). In water solution at pH 5.5, NMR studies of a β-(10-35)-$CONH_2$ fragment demonstrated a turn-strand-turn motif between His13-Val24 (Lee *et al*., 1995). Our earlier reports showed that below pH 3 in 60% TFE or SDS, the β-(1-28) peptide adopts a completely α-helical tertiary structure, while above pH 7, the first nine N-terminal residues unfold, leaving an α-helix at Tyr10-Lys28 (Zagorski & Barrow, 1992; Talafous *et al*., 1994; Marcinowski *et al*., 1998). Related NMR studies in dimethyl sulfoxide (DMSO) solution also revealed that the β-(1-28) adopts partly α-helical structure (Sorimachi & Craik, 1994). In contrast, CD and NMR studies of a β-(12-28) fragment established that a shorter Gln15-Lys28 segment becomes α-helical in SDS solution (Fletcher & Keire, 1997). An explanation for the shorter α-helix in the latter study may result from the absence of Glu11, which above pH 4 interacts favorably with the positively charged N terminus of the longer Tyr10-Val24 α-helix macrodipole (Zagorski & Barrow, 1992).

Altogether, the present results agree with most of these previous NMR studies, in that the β-peptide has a propensity for α-helical formation in membrane-mimicking conditions (TFE or SDS). Only minor differences were apparent (±0.02 ppm) from comparing the αH shifts of the present study to those for the β-(1-40) in 40% TFE (Sticht *et al*., 1995) and the β-(1-28) in SDS and 60% TFE (Zagorski & Barrow, 1992; Talafous *et al*., 1994; Marcinowski *et al*., 1998). The main differences relate to the relative lengths of the α-helices. For example, with the β-(1-28) in SDS at neutral pH the Tyr10-Lys28 segment was α-helical, which is four residues longer than the Tyr10-Val24 α-helix for the β-(1-40) and β-(1-42). This difference may be due to some secondary effect of the 29-42 region that is absent in the β-(1-28). One possibility is that the C-terminal Lys28-Ala42 α-helix forms first, and then subsequently directs the folding of the α-helix at Tyr10-Val24. Regarding the previous NMR studies of the β-(1-40) in 40% TFE (Sticht *et al*., 1995), the α-helices at Gln15-Asp23 and Ile31-Met35 are close to the best-fit regions of the β-(1-42). These differences may be due to the effect of TFE *versus* micelles, in that the micelles are better in stabilizing the α-helices and also in preventing aggregation into β-sheet structures. For the studies in 40% TFE, it was reported that some peptide precipitation took place after several days (Sticht *et al*., 1995), which suggests that the β-(1-40) may have been partly pre-aggregated. Here, our NMR solutions were generally stable for several months with no peptide precipitation.

Proximity of the β-peptide at the micelle surface

The present NMR data indicates that the β-(1-42) peptide remains on the micelle surface and does not become imbedded into the hydrophobic interior. First, the extremely rapid NH → ND exchange rates (within 30 minutes) support a surface location, since if the peptide were located inside the micelle, then the NH signals should exchange at slower rates (see, for example Van

de Ven *et al*., 1993). Second, the irregular pattern of the NH-temperature coefficients is consistent with a surface location, since if a peptide segment were located in the hydrophobic interior, then a long stretch of invariable coefficients should be observed. Such a pattern was seen for the smaller, non-native β-(25-35) peptide in SDS, where the C-terminal Ile32-Met35 segment had reduced coefficients relative to the N-terminal region (Kohno *et al*., 1996). Third, TOCSY spectra obtained with the spin-labeled 12-doxylstearic acid showed no line broadening, indicative of a surface location. In contrast, comparable spin-labeled studies of PhoE signal peptides in SDS showed selective and significant line broadening, consistent a buried location of certain residues in the micelle interior (Chupin *et al*., 1995). Fourth, recent work from our laboratory established that the His side-chains have elevated pKa values in SDS solution (Clancy, E. H. & M.G.Z., unpublished results), which supports electrostatic binding to the negatively charged sulfate groups at the SDS surface (Van Den Hooven *et al*., 1996). Fifth, the line widths of the NMR resonances are smaller than would be expected for a β-(1-42)/micelle complex that would be approximately 15 kDa (Henry & Sykes, 1994). The narrower line widths are indicative of conformational mobility at the micelle surface. For example, differences were seen with the bacteriophage M13 coat protein, in that significantly narrower line widths were found for residues at the micelle surface compared to residues located in the central rigid micelle spanning α-helix (Van de Ven *et al*., 1993).

The above interpretation seems plausible and consistent with the interaction of other proteins with micelles, since it avoids the thermodynamically unfavorable implication of burying, for example, the hydrophobic C terminus into the micelle interior. Recent studies with a mixture of neutral and negatively charged bilayer vesicles showed that the α-helical structure for the β-(1-40) does not penetrate into hydrophobic vesicle interior, and instead binds electrostatically to the outer negatively charged headgroups without penetration between the polar groups (Terzi *et al*., 1997). These results are consistent with the present findings in micelle solution. Nevertheless, because it has also been established that the β-peptide disrupts membranes containing acidic lipids (McLaurin & Chakrabartty, 1996, 1997) and that the 29-42 region has fusogenic properties (Pillot *et al*., 1996), it may happen that the hydrophobic C terminus undergoes rapid movement, inside and outside the micelle interior, in a manner that would not reduce the NH → ND exchange rates, maintain uniform NH temperature coefficients, or become broadened by a spin label. Additional NMR relaxation measurements using ^{13}C and ^{15}N labeled β-(1-42) are currently being explored to investigate these possibilities (Williams *et al*., 1996).

Mechanism of β-amyloidosis and membrane-bound β-(1-42) as a therapeutic target for β-amyloid inhibition

Shown in Figure 10 is a hypothetical model for the association of the β-(1-42) peptide with the SDS micelle and the aggregation into β-sheet structures. This mechanism takes into account the present results and work from other laboratories. The model emphasizes a conformationally driven mechanism, in which the three major solution structures of the β-peptide coexist in equilibrium: random coil (monomeric), α-helix (monomeric), and β-sheet (oligomeric).

After proteolysis from APP, the monomeric β-(1-42) would presumably be unfolded and adopt a random coil conformation (Figure 10). The random coil structure may undergo further proteolysis, with shorter and more soluble products being excreted. However, even at the low, nano to picomolar physiological concentration ranges (Gravina *et al*., 1995; Southwick *et al*., 1996), monomeric β-(1-42) molecules can converge and aggregate into stable oligomers (Podlisny *et al*., 1998). These β-aggregation processes (random coil → β-sheet) can be accelerated by brain micro-environmental changes that include higher peptide concentrations, decreases in pH (Barrow & Zagorski, 1991; Fraser *et al*., 1991; Burdick *et al*., 1992), or attachment of the β-peptide to metals or small amounts of racemized (Tomiyama *et al*., 1994) and/or preaggregated peptide that can act as a seed for precipitation (Jarrett & Lansbury, 1993). Some of the other components that induce aggregation include glycosaminoglycans (Snow & Wight, 1989; Brunden *et al*., 1993), zinc (Mantyh *et al*., 1993; Bush *et al*., 1994), Apo-E (Strittmatter *et al*., 1993; Ma *et al*., 1994; Evans *et al*., 1995; Soto *et al*., 1995c), glycation (Smith *et al*., 1994; Vitek *et al*., 1994), or NACP (non-Aβ protein component precursor; Yoshimoto *et al*., 1995).

Alternatively, if monomeric β-(1-42) encounters a hydrophobic micro-environment, similar to the SDS micelle, then a more stable and predominantly α-helical structure should form. As discussed before, this event may occur in human plasma or cerebrospinal fluid when the β-peptide becomes attached to lipoproteins, albumin, ApoJ, α_2-macroglobuln, or transthyretin (Schwarzman *et al*., 1994; Matsubara *et al*., 1995; Biere *et al*., 1996; Du *et al*., 1998). A recent study using synchrotron FT-IR microspectroscopy showed that the β-peptide adopts significant quantities of α-helical structure in the brain grey matter (Choo *et al*., 1996). Most likely, the α-helical structure is non-toxic, since it is monomeric, ordered, and very soluble (Farhangrazi *et al*., 1997). Nonetheless, it should be kept in mind that a lipid-bound α-helical structure for the β-peptide has yet to be detected in plasma or cerebrospinal fluid.

When unbound to the SDS micelle or a related biological lipid, the α-helical conformation can unfold to random coil structure (α-helix → random

coil) or aggregate into β-sheet structures (α-helix → β-sheet). Related conversions for other peptides and proteins (Dunker *et al*., 1982; Batenburgh *et al*., 1988; Fan *et al*., 1993; Graf v. Stosch *et al*., 1995; Shiraki *et al*., 1995), including peptide segments of the prion proteins (Nguyen *et al*., 1995; Zhang *et al*., 1995) are well documented. When the aggregation reaches a critical mass, the β-sheet structure precipitates as amyloid and reconversion back to the soluble random coil or α-helical structures is not possible (Barrow *et al*., 1992; Tomski & Murphy, 1992; Shen & Murphy, 1995). The mechanisms whereby the β-sheet structure exerts its neurotoxicity remain unknown (Sayre *et al*., 1997). Recent data suggests that soluble β-sheet oligomers are toxic (Roher *et al*., 1996; Garzon-Rodriguez *et al*., 1997; Lambert *et al*., 1998), with the larger amyloid plaques further disrupting neuronal circuitry. It is well known that monomeric and oligomeric species of β-peptide exist in equilibrium in aqueous solution and in tissue culture medium (Pike *et al*., 1991; Knauer *et al*., 1992; Esler *et al*., 1996b; Johnstone *et al*., 1996; Huang *et al*., 1997). It may happen that such soluble β-sheet structures produced before the plaque are, likewise, resistant to proteolysis, similar to soluble peptide segments of the amyloid forming prion proteins (Zhang *et al*., 1995).

Major research efforts focus on identifying inhibitors of β-amyloidosis (Lansbury, 1997). In fact, numerous studies have already uncovered β-amyloid inhibitors that may also prevent the associated neurotoxicity, which include Congo red (Lorenzo & Yankner, 1994; Brining, 1997; Podlisny *et al*., 1998), transthyretin (Schwarzman *et al*., 1994), apolipoproteins (Evans *et al*., 1995; Matsubara *et al*., 1996; Wood *et al*., 1996a), site-directed monoclonal antibodies (Solomon *et al*., 1997), melatonin (Pappolla *et al*., 1998), and short peptide fragments that presumably bind to the Lys16-Leu17-Val18-Phe19-Phe20 β-peptide region (Ghanta *et al*., 1996; Soto *et al*., 1996; Tjernberg *et al*., 1996). However, the therapeutic potential of these compounds is somewhat limited, due to the lack of detailed structural data about their binding to the β-peptide. Such structural information would greatly reduce the time required for the development of more appropriate analogs with greater specificity and capacity to cross the blood-brain barrier. In this regard, we believe that the α-helical structure provides an appropriate target for the design of amyloid inhibitors, since it is monomeric, stable, and suitable for modern structure-based drug design methods (Craik, 1996). As for the nicotine-inhibition to β-amyloidosis (Salomon *et al*., 1996), the NMR work established that nicotine binds to the His13 and His14 side-chains of the Tyr10-Val24 α-helix, and this prevented an α-helix → β-sheet conversion and β-amyloid precipitation. As discussed before, an interesting feature of the β-(1-42) tertiary structure is the relative proximity of the predominantly polar, charged Tyr10-Val24 α-helix and the mostly hydrophobic Lys28-Ala42 α-helix. A possible amyloid inhibitor could be designed with charged and neutral ends, which may bind more effectively to the Tyr10-Val24 and the Lys28-Ala42 α-helices, respectively (Figure 10). Such binding processes could stabilize the α-helices and prevent their rearrangement to the β-sheet, thus slowing down amyloidosis. In view of the lack of any effective treatments for AD, this approach may be an important prerequisite to a more rapid development of appropriate analogs to prevent amyloid formation.

Conclusions

The present study established that the SDS micelle encourages formation of predominantly α-helical structure for the β-peptide, that does not become inbedded into the micelle interior. Upon interaction with a naturally, charged membrane, the β-peptide region would be expected to initially adopt α-helical structure that does not insert into the hydrocarbon interior. Such stabilization may be critical to preventing an α-helix (soluble, monomeric) → β-sheet (insoluble amyloid deposit, toxic) conformational transition from occurring in the brains of AD patients. Although the structure obtained herein is different than what would be seen in the amyloid plaque, it has relevance for the association of the β-peptide with cellular membranes or lipoproteins and is, therefore, a structure that one would want to stabilize by pharmacological means as a potential therapeutic target.

Materials and Methods

Peptide purification

The primary amino acid sequence for the amyloid β-(1-42) peptide is the following: H_3N^+-D^1-A-E-F-R^5-H-D-S-G-Y^{10}-E-V-H-H-Q^{15}-K-L-V-F-F^{20}-A-E-D-V-G^{25}-S-N-K-G-A^{30}-I-I-G-L-M^{35}-V-G-G-V-V^{40}-I-A^{42}-COO^-. The amyloid β-(1-40) peptide has the identical sequence, except that the last two C-terminal residues (Ile41 and Ala42) are absent. Both peptides were purchased unpurified (Anaspec, Inc.), and then purified by high-performance liquid chromatography (HPLC) using a Millipore model 600E HPLC system, equipped with a Zorbax-300 bonded silica column (Rockland Technologies, Inc.), column heater (model 1233, Eldex, Inc.) and controller (CH-150, Eldex, Inc.). The solvent system consisted of a linear gradient of 20%-80% acetonitrile and 0.1%-0.08% trifluoroacetic acid (TFA) in water, which was heated to 55 °C to improve peak resolution and purity (Boyes, 1995). Peptide identity, verified by mass spectrometry (MS) and NMR, had purity levels greater than 85% (Jao *et al*., 1997).

Sample preparation

The solvents TFA and hexafluoroisopropanol (HFIP) were distilled under an inert atmosphere of nitrogen (N_2) and stored in opaque bottles at 5 °C. The perdeuterated SDS-d_{25}, ethylenediamine tetraacetic acid (Na_2EDTA-d_{12}), 3-(trimethylsilyl)propionate-2,2,3,3-d_4 (TSP), and the solvent ^2H_2O were obtained from Isotec, Inc. or Cam-

bridge Isotopes, Inc. The 12-doxylstearic acid was obtained from Sigma, Inc., and the solvent H_2O was distilled, HPLC grade that was essentially free of most organic and inorganic contaminants. Because the β-(1-40) and β-(1-42) peptides aggregate in the acetonitrile-water used for HPLC purification (Shen & Murphy, 1995), after purification and solvent removal, the dry purified peptides adopt mixtures of structures (α-helix, random coil, and β-sheet) and aggregation states (Soto *et al*., 1995b). This property greatly affects their solubility and the ability to obtain reproducible NMR measurements. To overcome these problems, we first pretreated the dry peptides with neat TFA (Jao *et al*., 1997). This procedure was performed on all peptide samples before they were dissolved in the buffered aqueous solution for NMR measurements.

The β-(1-40) and β-(1-42) peptide solutions (0.60 ml) were prepared at concentrations of 0.1-1.4 mM. The solvent free, TFA pretreated peptides were first dissolved in HFIP-d_2 (0.10 ml), followed by the addition of an aliquot (0.50 ml) of an SDS-d_{25} solution in water that also contained 20 mM sodium phosphate buffer at pH 7.2, 0.05 mM Na_2EDTA-d_{12}, 0.05 mM sodium azide (NaN_3), and 0.05 mM TSP. The latter three components were included to remove trace metal ions, prevent microbial growth, and provide an internal chemical shift reference at 0 ppm, respectively. The small amount of HFIP (10-15% by volume) in the final SDS-water solution does not influence the secondary structure, as determined by comparing CD and NMR spectra with and without the HFIP. The SDS-d_{25} concentration was kept high relative to the peptide concentration, so that it was well above 8 mM (the critical micelle concentration) and also above the average aggregation number (Henry & Sykes, 1994). The pH values were measured at room temperature and corrections for isotope effects or for the presence of HFIP-d_2 and SDS-d_{25} were not performed, since control experiments showed that these substances did not significantly alter the pH.

Nuclear magnetic resonance spectroscopy

All ^1H NMR spectra were obtained at 600 MHz using a Varian UnityPlus-600 spectrometer. The probe temperatures were calibrated using dry methanol and dry dimethyl sulfoxide (Van Geet, 1970). The NMR data were transferred to Indigo-XS24-R4000 (Silicon Graphics, Inc.) computer workstations and processed using the FELIX program (version 95.0, Biosym, Inc.).

The 2D NMR experiments included the NOESY (Kumar *et al*., 1980), and the clean TOCSY (Griesinger *et al*., 1988), the latter using a DIPSI isotropic mixing pulse sequence (Bax & Davis, 1985; Shaka *et al*., 1988). For the TOCSY and NOESY, the mixing times were 20-70 ms and 120-270 ms, respectively. Depending on the acquisition and mixing times, the total recycle delay between scans was 1.5-2.0 seconds. All experiments were obtained with 2048 or 4096 complex points in the F_2 dimension and 128-256 complex increments in the F_1 dimension each consisting 40-118 scans. The number of scans and increments was largely dependent on the peptide concentration, with more scans and less increments being acquired for more dilute samples. The carrier was placed in the center of the spectrum at the position of the water signal. Before Fourier transformation, the spectra were multiplied by a Lorentzian-to Gaussian window function in F_2, and a 80-90° phase-shifted sinebell or sinebell squared in F_1. Baseline roll was reduced by careful adjustment of the intensity of the first points in F_2 and F_1, and by the application of a FLATT baseline correction of the rows in the final 2D matrix (Güntert & Wüthrich, 1992).

To check for the possibility of αH and NH signal loss from water presaturation at pH 7.2, NOESY experiments were acquired with different methods to suppress the water signal, which included the standard presaturation, the Jump-Return sequence (Plateau & Gueron, 1982), and the WATERGATE pulse field gradient technique (Piotto *et al*., 1992; Kay, 1995). All three techniques gave comparable results, demonstrating that there was no detectable signal loss by the presaturation method.

The amide-NH temperature coefficients were obtained from NOESY spectra at 15.0, 20.0, 25.0 and 30.0 °C. The temperature coefficients ($-\Delta\delta/\Delta T$, ppb) were taken as the slopes from a least-squares computer fitted lines of the chemical shifts against temperature. For the NH-exchange experiments, a sample of β-(1-42) in water with SDS-d_{25} was lyophilized to dryness, re-dissolved in ^2H_2O. Both 1D and 2D NMR data were acquired at probe temperatures of 12 °C and at different time intervals since sample dissolution. To determine whether the β-peptides were located in the interior or exterior of the SDS micelle, the effect of the spin-labeled 12-doxylstearic acid on the ^1H signals was investigated. Two TOCSY spectra for a 0.70 mm β-(1-40) solution (0.5 ml) in ^2H_2O containing 66 mM SDS-d_{25} at pH 7.3 were obtained: one spectrum before and the other spectrum after the addition of an aliquot (10 μl) of a 37 mM 12-doxylstearic acid solution in methanol-d_4. The molar ratios of peptide to micelle and peptide to 12-doxylstearic acid were 1.0:1.0 and 1.0:0.9, respectively. To prevent air-oxidation of the spin label, the NMR solutions were degassed and covered with a blanket of N_2. The intensities of the TOCSY cross-peaks in the presence and absence of spin-labeled acid were compared.

Distance restraints

The NOESY cross-peak intensities (mixing time 270 ms, 20.0 °C) were determined with the FELIX program (version 97.0, Biosym, Inc.) and converted to distance restraints. The NOESY spectra obtained at mixing times of 120 and 270 ms were nearly identical, and any additional weak NOEs that were present in the longer mixing time NOESY were not used as restraints. From the NOESY data, 121 intra-residue and 125 inter-residue restraints (84 sequential and 41 medium range) were obtained. The intra-residue restraints with redundant covalent limits were discarded by the distance geometry (DGII) programs (Biosym, Inc.). The NOEs classified as strong, medium, and weak corresponded to interproton distance restraints of 1.8-2.5, 1.8-3.5, and 1.8-5.0 Å, respectively. Cross-peaks with greater than 30% overlapped area were used as qualitative upper bound restraints of 1.8-5.0 Å, and pseudoatom corrections were used for degenerate peaks. In situations where prochiral constituents were spectroscopically distinguishable, but not assigned stereospecifically, the resonance was assigned arbitrarily and allowed to freely interchange their chiralities during the structure calculations. Additional 0.5 and 1.0 Å upperbound limits were applied to intra- and inter-residue NOEs involving methyl peaks. Although the amide-NH temperature coefficients established the presence of some reasonably strong hydrogen bonds, hydrogen bond constraints were

not employed, since they can sometimes bias the structure refinement.

Structure calculations

Structures were computed using a well-established DGII method (Havel, 1991), which was part of the NMR-refine module of the INSIGHT II program (version 95.0, Biosym, Inc.). Before starting the DGII calculations, an extended linear chain of the β-(1-42) peptide was constructed using the BIOPOLYMER module and then minimized with the DISCOVER program (version 2.97, Biosym, Inc.). The DGII protocol includes bound smoothing, in which triangular inequality limits are determined for distance geometry, followed by random metrization with the coordinates and the appropriate distances obtained by angular embedding and majorization procedures. The final structures are optimized by simulated annealing and conjugate gradient minimization procedures. For the β-(1-42), an initial set of 30 structures was calculated using 246 distance restraints enforced with a force constant of 1 kcal/mol Å^2. After the initial calculations, the restraint file was checked to make certain adjustments and to identify misassignments. This step was repeated several times before the final calculations. Of the 30 structures, 12 were discarded before further minimization because of the large constraint violations (greater than 0.35 Å). The remaining 18 structures were further minimized in the DISCOVER module using a CVFF forcefield with an enforced dielectric constant of 1, side-chains with their expected charges at pH 7.2, and the distance restraints enforced with a force constant of 30 kcal/mol Å^2. All the force constants were scaled to 1.0. The first stage of minimization consisted of 200 iterations of steepest descent, followed by 2000 iterations of conjugate gradients minimizations to reduce the repulsive non-bonded contacts. These procedures reduced the final average energies from an initial 2698 kcal/mol down to 398 kcal/mol.

Acknowledgments

Supported in part by grants from the National Institutes of Health (AG-08992-06 and AG-14363-01), the Smokeless Tobacco Research Council, Philip Morris, U.S.A., and a Faculty Scholars Award from the Alzheimer's Association to M.G.Z. (FSA-94-040). The 600 MHz NMR spectrometer was purchased with funds provided by the National Science Foundation, the National Institutes of Health, and the State of Ohio. We would like to thank Anita Hong (Anaspec, Inc.), Mark Smith and Witold Surewicz for helpful discussions.

References

Arispe, N., Pollard, H. B. & Rojas, E. (1993). Giant multilevel cation channels formed by Alzheimer disease amyloid β-protein (AβP-1-40) in bilayer membranes. *Proc. Natl Acad. Sci. USA*, **90**, 10573-10577.

Avdulov, N., Chochina, S. V., Igbavboa, U., O'Hare, E. O., Schroeder, F., Cleary, J. P. & Wood, W. G. (1997). Amyloid β-peptides increase annular and bulk fluidity and induce lipid peroxidation in brain synaptic plasma membranes. *J. Neurochem.* **68**, 2086-2091.

Barrow, C. J. & Zagorski, M. G. (1991). Solution structures of β peptide and its constituent fragments: relation to amyloid deposition. *Science*, **253**, 179-182.

Barrow, C. J., Yasuda, A., Kenny, P. T. M. & Zagorski, M. G. (1992). Solution conformations and aggregational properties of synthetic amyloid β-peptides of Alzheimer's disease. Analysis of circular dichroism spectra. *J. Mol. Biol.* **225**, 1075-1093.

Batenburgh, A. M., Brasseur, R., Ruysschaert, J.-M., van Scharrenburgh, G. J. M., Slotboom, A. J., Demel, R. A. & Kruijff, B. d. (1988). Characterization of the interfacial behavior and structure of the signal sequence of *Escherichia coli* outer membrane pore protein PhoE. *J. Biol. Chem.* **263**, 4202-4207.

Bax, A. & Davis, D. G. (1985). MLEV-17 based two-dimensional homonuclear magnetization transfer spectroscopy. *J. Magn. Reson.* **65**, 355-360.

Biere, A. L., Ostaszewski, B., Stimson, E. R., Hyman, B. T., Maggio, J. E. & Selkoe, D. J. (1996). Amyloid β-peptide is transported on lipoproteins and albumin in human plasma. *J. Biol. Chem.* **271**, 32916-32922.

Boyes, B. E. (1995). *14th American Peptide Symposium*, Columbus, OH.

Brining, S. K. (1997). Predicting the *in vitro* toxicity of synthetic beta-amyloid (1-40). *Neurobiol. Aging*, **18**, 581-589.

Brunden, K. R., Richter-Cook, N. J., Chaturvedi, N. & Frederickson, R. C. A. (1993). pH-dependent binding of synthetic β-amyloid peptides to glycosaminoglycans. *J. Neurochem.* **61**, 2147-2154.

Burdick, D., Soreghan, B., Kwon, M., Kosmoski, J., Knauer, M., Henschen, A., Yates, J., Cotman, C. & Glabe, C. (1992). Assembly and aggregational properties of synthetic Alzheimer's A4/β amyloid peptide analogs. *J. Biol. Chem.* **267**, 546-554.

Bush, A. I., Pettingell, W. H., Multhaup, G., Paradis, M., Vonsattel, J.-P., Gusella, J. F., Beyreuther, K., Masters, C. L. & Tanzi, R. E. (1994). Rapid induction of Alzheimer Aβ amyloid formation by zinc. *Science*, **265**, 1464-1467.

Case, D. A. & Wright, P. E. (1993). Determination of high-resolution NMR structures of proteins. In *NMR of Proteins* (Clore, G. M. & Gronenborn, A. M., eds), CRC, Ann Arbon.

Choo, L.-P. I., Wetzel, D. L., Halliday, W. C., Jackson, M., LeVine, S. M. & Mantsch, H. H. (1996). *In situ* characterization of β-amyloid in Alzheimer's diseased tissue by synchroton Fourier transform infrared microspectroscopy. *Biophys. J.* **71**, 1672-1679.

Chupin, V., Kilian, J. A., Breg, J., de Jongh, H. H. J., Boelens, R., Kaptein, R. & Kruijff, B. D. (1995). PhoE signal peptide inserts into micelles as a dynamic helix-break-helix structure, which is modulated by the environment. A two-dimensional ^{1}H NMR study. *Biochemistry*, **34**, 11617-11624.

Coles, M., Bicknell, W., Watson, A. A., Fairlie, D. P. & Craik, D. J. (1998). Solution structure of amyloid beta-peptide(1-40) in a water-micelle environment. Is the membrane-spanning domain where we think it is?. *Biochemistry*, **37(31)**, 11064-11077.

Craik, D. J. (1996). *NMR in Drug Design*, CRC Press, Boca Raton.

Du, Y., Bales, K. R., Dodel, R. C., Liu, X., Glinn, M. A., Horn, J. W., Little, S. P. & Paul, S. M. (1998). α_2-Macroglobulin attenuates β-amyloid peptide 1-40 fibril formation and associated neurotoxicity of cultured fetal rat cortical neurons. *J. Neurochem.* **70(3)**, 1182-1188.

Dunker, A. K., Fodor, S. P. A. & Williams, R. W. (1982). Lipid-dependent structural changes of an amphomorphic membrane protein. *Biophys. J.* **37**, 201-203.

Dyson, H. J., Rance, M., Houghten, R. A., Lerner, R. A. & Wright, P. E. (1988). Folding of immunogenic peptide fragments of proteins in water solution. I. sequence requirements for the formation of a reverse turn. *J. Mol. Biol.* **201**, 161-200.

Esler, W. P., Stimson, E. R., Ghilardi, J. R., Lu, Y.-A., Felix, A. M., Vinters, H. V., Mantyh, P. W., Lee, J. P. & Maggio, J. E. (1996a). Point substitution in the central-hydrophobic cluster of a human β-amyloid congener disrupts peptide folding and abolishes plaque competence. *Biochemistry*, **35**, 13914-13921.

Esler, W. P., Stimson, E. R., Ghilardi, J. R., Vinters, H. V., Lee, J. P., Mantyh, P. W. & Maggio, J. E. (1996b). *In vitro* growth of Alzheimer's disease β-amyloid plaques displays first-order kinetcis. *Biochemistry*, **35**, 749-757.

Evans, K. C., Berger, E. P., Cho, C.-G., Weisgraber, K. H. & Lansbury, P. T. (1995). Apolipoprotein E is a kinetic but not a thermodynamic inhibitor of amyloid formation: implications for the pathogenesis and treatment of Alzheimer's disease. *Proc. Natl Acad. Sci. USA*, **92**, 763-767.

Fan, P., Bracken, C. & Baum, J. (1993). Structural characterization of mMonellin in the alcohol-denatured state by NMR: evidence for β-sheet to α-helix conversion. *Biochemistry*, **32**, 1573-1582.

Farhangrazi, Z. S., Ying, H., Bu, G., Dugan, L. L., Fagan, A. M., Choi, D. W. & Holtzman, D. M. (1997). High density lipoprotein decreases β-amyloid toxicity in cortical cell culture. *NeuroReport*, **8**, 1127-1130.

Fletcher, T. G. & Keire, D. A. (1997). The interaction of β-amyloid protein fragment (12-28) with lipid environments. *Protein Sci.* **6**, 666-675.

Fraser, P. E., Nguyen, J. T., Surewicz, W. K. & Kirschner, D. A. (1991). pH dependent structural transitions of Alzheimer amyloid peptides. *Biophys. J.* **60**, 1190-1201.

Garzon-Rodriguez, W., Sepulveda-Becerra, M., Milton, S. & Glabe, C. G. (1997). Soluble amyloid Aβ-(1-40) exists as a stable dimer at low concentrations. *J. Biol. Chem.* **272**, 21037-21044.

Geetha, V. & Munson, P. J. (1997). Linkers of secondary structures in proteins. *Protein Sci.* **6**, 2538-2547.

Ghanta, J., Shen, C.-L., Kiessling, L. L. & Murphy, R. M. (1996). A strategy for designing inhibitors of β-amyloid toxicity. *J. Biol. Chem.* **271**, 29525-29528.

Good, T. A. & Murphy, R. M. (1995). Aggregation state-dependent binding of β-amyloid peptide to protein and lipid components of rat cortical homogenates. *Biochem. Biophys. Res. Commun.* **207**, 209-215.

Good, T. A. & Murphy, R. M. (1996). Effect of β-amyloid block of the fast-inactivating K^+ channel on intracellular Ca^{2+} and excitability in a modeled neuron. *Proc. Natl Acad. Sci. USA*, **93**, 15130-15135.

Graf v. Stosch, A., Jiménez, M. A., Kinzel, V. & Reed, J. (1995). Solvent polarity-dependent structural refolding: a CD and NMR study of a 15 residue peptide. *Proteins: Struct. Funct. Genet.* **23**, 196-203.

Gravina, S. A., Ho, L., Eckman, C. B., Long, K. E., Otvos, L., Jr, Younkin, L. H., Suzuki, N. & Younkin, S. G. (1995). Amyloid β protein (Aβ) in Alzheimer's disease brain. *J. Biol. Chem.* **270**, 7013-7016.

Griesinger, C., Otting, G., Wüthrich, K. & Ernst, R. R. (1988). Clean TOCSY for ^1H spin system identification in macromolecules. *J. Am. Chem. Soc.* **110**, 7870-7872.

Güntert, P. & Wüthrich, K. (1992). FLATT-a new procedure for high-quality baseline correction of multidimensional NMR spectra. *J. Mag. Res.* **96**, 403-407.

Hardy, J. (1997). Amyloid, the presenilins and Alzheimer's disease. *Trends Neurosci.* **20**, 154-159.

Harper, J. D. & Lansbury, P. T. (1997). Models of amyloid seeding in Alzheimer's disease and scrapie: mechanistic truths and physiological consequences of the time-dependent solubility of amyloid proteins. *Annu. Rev. Biochem.* **66**, 385-407.

Havel, T. (1991). An evaluation of computational strategies for use in the determination of protein structures from distance constraints obtained by nuclear magentic resonance. *Prog. Biophys. Mol. Biol.* **56**, 43-78.

Henry, G. D. & Sykes, B. D. (1994). Methods to study membrane protein structure in solution. *Methods Enzymol.* **239**, 520-534.

Hilbich, C., Kisters-Woike, B., Reed, J., Masters, C. L. & Beyreuther, K. (1991). Aggregation and secondary structure of synthetic amyloid βA4 peptides of Alzheimer's disease. *J. Mol. Biol.* **218**, 149-163.

Hilbich, C., Kisters-Woike, B., Reed, J., Masters, C. L. & Beyreuther, K. (1992). Substitutions of hydrophobic amino acids reduce the amyloidogenicity of Alzheimer's disease βA4 peptides. *J. Mol. Biol.* **228**, 4609-473.

Huang, T. H. J., Fraser, P. E. & Chakrabartty, A. (1997). Fibrillogenesis of Alzheimer Aβ peptides studied by fluorescence energy transfer. *J. Mol. Biol.* **269**, 214-224.

Iqbal, K., Winblad, B., Nishimura, T., Takeda, M. & Wisniewski, H. M. (1997). *Alzheimer's Disease: Biology, Diagnosis, and Therapeutics*, John Wiley & Sons, Ltd, New York.

Jao, S.-C., Ma, K., Talafous, J., Orlando, R. & Zagorski, M. G. (1997). Trifluoroacetic acid pretreatment reproducibly disaggregates the amyloid β-peptide. *Int. J. Exp. Clin. Invest.* **4**, 240-252.

Jarrett, J. T. & Lansbury, P. T. (1993). Seeding ''one-dimensional crystallization'' of amyloid: a pathogenic mechanism in Alzheimer's disease and scrapie? *Cell*, **73**, 1055-1058.

Johnstone, E. M., Babbey, L. E., Stepenson, D., Paul, D. C., Santerre, R. F., Clemens, J. A., Willians, D. C. & Little, S. P. (1996). Nuclear and cytoplasmic localization of the β-amyloid peptide (1-43) in transfected 293 cells. *Biochem. Biophys. Res. Commun.* **220**, 710-718.

Kawahara, M., Arispe, N., Kuroda, Y. & Rojas, E. (1997). Alzheimer's disease amyloid β-protein form Zn^{2+}-sensitive, cation-selective channels across excised membrane patches from hypothalamic neurons. *Biophys. J.* **73**, 67-75.

Kay, L. E. (1995). Pulsed field gradient multi-dimensional NMR methods for the study of protein structure and dynamics in solution. *Prog. Biophys. Mol. Biol.* **63**, 277-299.

Kirschner, D. A., Abraham, C. & Selkoe, D. J. (1986). X-ray diffraction from intraneuronal paired helical filaments and extraneuronal amyloid fibers in Alzheimer's disease indicates cross-β conformation. *Proc. Natl Acad. Sci. USA*, **83**, 503-507.

Klunk, W. E., Xu, C.-J., McClure, R. J., Panchalingam, K., Stanley, J. A. & Pettegrew, J. W. (1997). Aggregation of β-amyoid peptide is promoted by membrane phospholid metabolites elevated in Alzheimer's disease brain. *J. Neurochem.* **69**, 266-272.

Knauer, M., Soreghan, B., Burdick, D., Kosmoski, J. & Glabe, C. (1992). Intracellular accumulation and resistance to degradation of the Alzheimer amyloid A4/β protein. *Proc. Natl Acad. Sci. USA*, **89**, 7437-7441.

Kohno, T., Kobayashi, K., Maeda, T., Sato, K. & Takashima, A. (1996). Three-dimensional structures of the amyloid β peptide (25-35) in membrane-mimicking environment. *Biochemistry*, **35**, 16094-16104.

Koudinov, A. R., Koudinova, N. V., Kumar, A., Beavis, R. C. & Ghiso, J. (1996). Biochemical characterization of Alzheimer's soluble amyloid beta protein in human cerebrospinal fluid: association with high density lipoproteins. *Biochem. Biophys. Res. Commun.* **223**, 592-597.

Kumar, A., Ernst, R. R. & Wüthrich, K. (1980). A two-dimensional nuclear Overhauser enhancement (2D NOE) experiment for the elucidation of complete proton-proton cross relaxation networks in biological macromolecules. *Biochem. Biophys. Res. Commun.* **95**, 1-6.

Kuntz, I. D., Kosen, P. A. & Craig, E. C. (1991). Amide chemical shifts in many helices in peptides and proteins are periodic. *J. Am. Chem. Soc.* **113**, 1406-1408.

Lambert, M. P., Barlow, A. K., Chromy, B. A., Edwards, C., Freed, R., Liosatos, M., Morgan, T. E., Rozovsky, I., Trommer, B., Viola, K. L., Wals, P., Zhang, C., Finch, C. E., Krafft, G. A. & Klein, W. L. (1998). Diffusible, nonfibrillar ligands derived from Abeta1-42 are potent central nervous system neurotoxins. *Proc. Natl Acad. Sci. USA*, **95(11)**, 6448-6453.

Lansbury, P. T. (1997). Inhibition of amyloid formation: a strategy to delay the onset of Alzheimer's disease. *Curr. Opin. Chem. Biol.* **1(2)**, 260-267.

Lee, J. P., Stimson, E. R., Ghilardi, J. R., Mantyh, P. W., Lu, Y.-A., Felix, A. M., Llanos, W., Behbin, A., Cummings, M., van Criekinge, M., Timms, W. & Maggio, J. E. (1995). ^{1}H NMR of Aβ amyloid peptide congeners in water solution. Conformational changes correlate with plaque competence. *Biochemistry*, **34**, 5191-5200.

Levy-Lahad, E., Wasco, W., Poorkaj, P., Romano, D. M., Oshima, J., Pettingell, W. H., Yu, C.-E., Jondro, P. D., Schmidt, S. D., Wang, K., Crowley, A. C., Fu, Y.-H., Guenette, S. Y., Galas, D., Nemens, E., *et al*. (1995). Candidate gene for the chromosome 1 familial Alzheimer's disease locus. *Science*, **269**, 973-977.

Lorenzo, A. & Yankner, B. A. (1994). β-Amyloid neurotoxicity requires fibril formation and is inhibited by Congo red. *Proc. Natl Acad. Sci. USA*, **91**, 12243-12247.

Ma, J., Yee, A. H., Bryan Brewer, J., Das, S. & Potter, H. (1994). Amyloid-associated proteins α_1-antichymotrypsin and apolipoprotein E promote assembly of Alzheimer β-protein into filaments. *Nature*, **372**, 92-94.

Malinchik, S. B., Inouye, H., Szumowski, K. E. & Kirschner, D. A. (1998). Structural analysis of Alzheimer's β(1-40) amyloid: protofilament assembly of tubular fibrils. *Biophys. J.* **74**, 537-545.

Mantyh, P. W., Ghilardi, J. R., Rogers, S., DeMaster, E., Allen, C. J., Stimson, E. R. & Maggio, J. E. (1993). Aluminum, iron, and zinc ions promote aggregation of physiological concentrations of β-amyloid peptide. *J. Neurochem.* **61(3)**, 1171-1174.

Marcinowski, K. J., Shao, H., Clancy, E. L. & Zagorski, M. G. (1998). Solution structures of residues 1-28 of the amyloid β-peptide when bound to micelles. *J. Am Chem. Soc.*, **120**, 11082-11091.

Mason, R. P., Estermyer, J. D., Kelly, J. F. & Mason, P. E. (1996). Alzheimer's disease amyloid β peptide 25-35 is localized in the membrane hydrocarbon core: X-ray diffraction analysis. *Biochem. Biophys. Res. Commun.* **222**, 78-82.

Matsubara, E., Frangione, B. & Ghiso, J. (1995). Characterization of apoliproprotein J-Alzheimer's Aβ interaction. *J. Biol. Chem.* **270(13)**, 7563-7567.

Matsubara, E., Soto, C., Governale, S., Frangione, B. & Ghiso, J. (1996). Apolipoprotein J and Alzheimer's amyloid β solubility. *Biochem. J.* **316**, 671-679.

Mattson, M. P., Tomaselli, K. J. & Rydel, R. E. (1993). Calcium-destabilizing and neurodegenerative effects of aggregated β-amyloid peptide are attenuated by basic FGF. *Brain Res.* **621**, 35-49.

McDonnell, P. A. & Opella, S. J. (1993). Effect of detergent concentration on multidimensional solution NMR spectra of membrane proteins in micelles. *J. Magn. Reson. sect. B*, **102**, 120-125.

McLaurin, J. & Chakrabartty, A. (1996). Membrane disruption by Alzheimer β-amyloid peptides mediated through specific binding to either phospholipids or gangliosides. *J. Biol. Chem.* **271(43)**, 26482-26489.

McLaurin, J. & Chakrabartty, A. (1997). Characterization of the interactions of Alzheimer β-amyloid peptides with phospholipid membranes. *Eur. J. Biochem.* **245**, 355-363.

Nguyen, J., Baldwin, M. A., Cohen, F. E. & Prusiner, S. B. (1995). Prion protein peptides induce α-helix to β-sheet conformational transitions. *Biochemistry*, **34**, 4186-4192.

Nordstedt, C., Näslund, J., Tjernberg, L. O., Karlström, A. R., Thyberg, J. & Terenius, L. (1994). The Alzheimer's Aβ peptide develops protease resistance in association with its polymerization into fibrils. *J. Biol. Chem.* **269(49)**, 30773-30776.

Otvos, L. J., Szendrei, G. I., Lee, V. M. Y. & Mantsch, H. H. (1993). Human and rodent Alzheimer β-amyloid peptides acquire distinct conformations in membrane-mimicking solvents. *Eur. J. Biochem.* **211**, 249-257.

Papavoine, C. H. M., Konings, R. N. H., Hilbers, C. W. & van de Ven, F. J. M. (1994). Location of M13 coat protein in sodium dodecyl sulfate micelles as determined by NMR. *Biochemistry*, **33**, 12990-12997.

Pappolla, M., Bozner, P., Soto, C., Shao, H., Robakis, N. K., Zagorski, M. G., Frangione, B. & Ghiso, J. (1998). Inhibition of Alzheimer β-fibrillogenesis by melatonin. *J. Biol. Chem.* **273**, 7185-7188.

Pike, C., Walencewicz, A., Glabe, C. & Cotman, C. (1991). *In vitro* aging of β-amyloid protein causes peptide aggregation and neurotoxicity. *Brain Res.* **563**, 311-314.

Pike, C. J., Walencewicz-Wasserman, A. J., Kosmoski, J., Cribbs, D. H., Glabe, C. G. & Cotman, C. W. (1995). Structure-activity analysis of β-amyloid peptides: contributions of the β25-35 region to aggregation and neurotoxicity. *J. Neurochem.* **64**, 253-265.

Pillot, T., Marc, G., Vanloo, B., Talussot, C., Brasseur, R., Vandekerckhove, J., Rosseneu, M. & Lins, L. (1996). Fusogenic properties of the C-terminal domain of the Alzheimer β-amyloid peptide. *J. Biol. Chem.* **271(46)**, 28757-28765.

Piotto, M., Saudek, V. & Sklenar, V. (1992). Gradient-tailored excitation for single-quantum NMR spectroscopy of aqueous solutions. *J. Biomol. NMR*, **2**, 661-665.

Plateau, P. & Gueron, M. (1982). Exchangeable proton NMR without base-line distortion using new strong-pulse sequences. *J. Am. Chem. Soc.* **104**, 7310-7311.

Podlisny, M. B., Walsh, D. M., Amarante, P., Ostaszewski, B. L., Stimson, E. R., Maggio, J. E., Teplow, D. B. & Selkoe, D. J. (1998). Oligomerization of endogenous and synthetic amyloid β-protein at nanomolar levels in cell culture and stabilization of monomer by congo red. *Biochemistry*, **37**, 3602-3611.

Roher, A. E., Chaney, M. O., Kuo, Y.-M., Webster, S. D., Stine, W. B., Haverkamp, L. J., Woods, A. S., Cotter, R. J., Tuohy, J. M., Krafft, G. A., Bonnell, B. S. & Emmerling, M. R. (1996). Morphology and toxicity of Aβ-(1-42) dimer derived from neuritic and vascular amyloid deposits of Alzheimer's disease. *J. Biol. Chem.* **271**, 20631-20635.

Roses, A. D. (1995). Alzheimer's disease as a model of molecular gerontology. *J. NIH Res.* **7**, 51-56.

Salomon, A. R., Marcinowski, K. J., Friedland, R. P. & Zagorski, M. G. (1996). Nicotine inhibits amyloid formation by the β-peptide. *Biochemistry*, **35(42)**, 13568-13578.

Sayre, L. M., Zagorski, M. G., Surewicz, W. K., Krafft, G. A. & Perry, G. (1997). Mechanisms of neurotoxicity with amyloid β deposition and the role of free radicals in the pathogenesis of Alzheimer's disease. A critical appraisal. *Chem. Res. Toxicol.* **10**, 518-526.

Schwarzman, A. L., Gregori, L., Vitek, M. P., Lyubski, S., Strittmatter, W. J., Enghilde, J. J., Bhasin, R., Silverman, J., Weisgraber, K. H., Coyle, P. K., Zagorski, M. G., Talafous, J., Eisenberg, M., Saunders, A. M., Roses, A. D. & Goldgaber, D. (1994). Transthyretin sequesters amyloid β protein and prevents amyloid formation. *Proc. Natl Acad. Sci. USA*, **91**, 8368-8372.

Selkoe, D. J. (1994). Normal and abnormal biology of the β-amyloid precursor protein. *Annu. Rev. Neurosci.* **17**, 489-517.

Shaka, A. J., Lee, C. J. & Pines, A. (1988). Iterative schemes for bilinear operators: application to spin decoupling. *J. Magn. Reson.* **77**, 274-293.

Shen, C.-L. & Murphy, R. M. (1995). Solvent effects on self-assembly of β-amyloid peptide. *Biophys. J.* **69**, 640-651.

Shiraki, K., Nishikawa, K. & Goto, Y. (1995). Trifluoroethanol-induced stabilization of the α-helical structure of β-lactoglobulin: implication for non-hierarchical protein folding. *J. Mol. Biol.* **245**, 180-194.

Shoemaker, K. R., Kim, P. S., York, E. J., Stewart, J. M. & Baldwin, R. L. (1987). Tests of the helix dipole model for stabilization of α-helices. *Nature*, **326**, 563-567.

Simmons, L. K., May, P. C., Tomaselli, K. J., Rydel, R. E., Fuson, K. S., Brigham, E. F., Wright, S., Lieberburg, I., Becker, G. W., Brems, D. N. & Li, W. (1994). Secondary structure of β-amyloid peptide correlates with toxicity *in vitro*. *Mol. Pharmacol.* **45**, 373-379.

Smith, M. A. (1998). Alzheimer disease. *Internat. Rev. Neurobiol.* **42**, 1-54.

Smith, M. A., Taneda, S., Richey, P. L., Miyata, S., Yan, S.-D., Stern, D., Sayre, L. M., Monnier, V. M. & Perry, G. (1994). Advanced maillard reaction end products are associated with Alzheimer disease pathology. *Proc. Natl Acad. Sci. USA*, **91**, 5710-5714.

Snow, A. D. & Wight, T. N. (1989). Proteoglycans in the pathogenesis of Alzheimer's disease and other amyloidoses. *Neurobiol. Aging*, **10**, 481-497.

Solomon, B., Koppel, R., Frankel, D. & Hanan-Aharon, E. (1997). Disaggregation of Alzheimer β-amyloid by site-directed mAb. *Proc. Natl Acad. Sci. USA*, **94**, 4109-4112.

Sorimachi, K. & Craik, D. J. (1994). Structure determination of extracellular fragments of amyloid proteins involved in Alzheimer's disease. *Eur. J. Biochem.* **219**, 237-251.

Soto, C., Castano, E. M., Frangione, B. & Inestrosa, N. C. (1995a). The α-helical to β-strand transition in the amino-terminal fragment of the amyloid β-peptide modulates amyloid formation. *J. Biol. Chem.* **270(7)**, 3063-3067.

Soto, C., Castaño, E. M., Kumar, R. A., Beavis, R. C. & Frangione, B. (1995b). Fibrillogenesis of synthetic amyloid-β peptides is dependent on their initial secondary structure. *Neurosci. Letters*, **200**, 105-108.

Soto, C., Castaño, E. M., Prelli, F., Kumar, R. A. & Baumann, M. (1995c). Apoliprotein E increases the fibrillogenic potential of synthetic peptides derived from Alzheimer's, Gelsolin and AA amyloids. *FEBS Letters*, **371**, 110-114.

Soto, C., Kindy, M. S., Baumann, M. & Frangione, B. (1996). Inhibition of Alzheimer's ayloidosis by peptides that prevent β-sheet conformation. *Biohem. Biophys. Res. Commun.* **226**, 672-680.

Southwick, P. C., Yamagata, S. K., Echols, C. L., Higson, G. J., Neynaber, S. A., Parson, R. e. & Munroe, W. A. (1996). Assessment of amyloid β protein in cerebrospinal fluid as an aid in the diagnosis of Alzheimer's disease. *J. Neurochem.* **66(1)**, 259-265.

Sticht, H., Bayer, P., Willbold, D., Dames, S., Hilbich, C., Beyreuther, K., Frank, R. W. & Rösch, P. (1995). Structure of amyloid A4-(1-40)-peptide of Alzheimer's disease. *Eur. J. Biochem.* **233**, 293-298.

Strittmatter, W. J., Weisgraber, K. H., Huang, D. Y., Dong, L.-M., Salvesen, G. S., Pericak-Vance, M., Schmechel, D., Saunders, A. M., Goldgabr, D. & Roses, A. D. (1993). Binding of human apolipoprotein E to synthetic amyloid β-peptides: isoform-specific effects and implications for late-onset Alzheimer's disease. *Proc. Natl Acad. Sci. USA*, **90**, 8098-8102.

Talafous, J., Marcinowski, K. J., Klopman, G. & Zagorski, M. G. (1994). Solution structure of residues 1-28 of the amyloid β-peptide. *Biochemistry*, **33**, 7788-7796.

Teplow, D. B. (1998). Structural and kinetic features of amyloid β-protein fibrillogenesis. *Int. J. Exp. Clin. Invest.* **5**, 121-142.

Terzi, E., Hölzemann, G. & Seelig, J. (1995). Self-association of β-amyloid peptide (1-40) in solution and binding to lipid membranes. *J. Mol. Biol.* **252**, 633-642.

Terzi, E., Hölzemann, G. & Seelig, J. (1997). Interaction of Alzheimer β-amyloid peptide (1-40) with lipid membranes. *Biochemistry*, **36**, 14845-14852.

Tjernberg, L. O., Näslund, J., Lindqvist, F., Johansson, J., Karlström, A. R., Thyberg, J., Terenius, L. & Nordstedt, C. (1996). Arrest of β-amyloid fibril formation by a pentapeptide ligand. *J. Biol. Chem.* **271(15)**, 8545-8548.

Tomiyama, T., Asano, S., Furiya, Y., Shirasawa, T., Endo, N. & Mori, H. (1994). Racemization of Asp^{23} residue affects the aggregation properties of Alzhei-

mer amyloid β protein analogues. *J. Biol. Chem.* **269(14)**, 10205-10208.
Tomski, S. J. & Murphy, R. M. (1992). Kinetics of aggregation of synthetic β-amyloid peptide. *Arch. Biochem. Biophys.* **294**, 630-638.
Van de Ven, F. J. M., Van Os, J. W. M., Aelen, J. M. A., Wymenga, S. S., Remerowski, M. L., Konings, R. N. H. & Hilbers, C. W. (1993). Assignment of ^{1}H, ^{15}N, and ^{13}C resonances in detergent solubilized M13 coat protein *via* multinuclear multidmensional NMR: a model for the coat protein monomer. *Biochemistry*, **32**, 8322-8328.
Van Den Hooven, H. W., Spronk, C. A. E. M., Van De Kamp, M., Konings, R. N. H., Hilbers, C. W. & Van De Ven, F. J. M. (1996). Surface location and orientation of the lantibiotic nisin bound to membrane-mimicking micelles of dodecylphosphocholine and of sodium dodecylsulphate. *Eur. J. Biochem.* **235(394-403)**, 394-403.
Van Geet, A. L. (1970). Calibration of methanol nuclear magnetic resonance thermometer at low temperature. *Anal. Chem.* **42**, 679-680.
Vitek, M. P., Bhattacharya, K., Glendening, J. M., Stopa, E., Vlassara, H., Bucala, R., Manogue, K. & Cerami, A. (1994). Advanced glycation end products contribute to amyloidosis in Alzheimer disease. *Proc. Natl Acad. Sci. USA*, **91**, 4766-4770.
Williams, K. A., Farrow, N. A., Deber, C. M. & Kay, L. E. (1996). Structure and dynamics of bacteriophage IKe major coat protein in MPG micelles by solution NMR. *Biochemistry*, **35**, 5145-5157.
Wishart, D. S., Sykes, B. D. & Richards, F. M. (1992). The chemical shift index: a fast and simple method for the assignment of protein secondary structure through NMR spectroscopy. *Biochemistry*, **31**, 1647-1651.
Wishart, D. S., Bigam, C. G., Holm, A., Hodges, R. S. & Sykes, B. D. (1995). ^{1}H, ^{13}C, and ^{15}N random coil NMR chemical shifts of the common amino acids. I. Investigations of nearest-neighbor effects. *J. Biomol. NMR*, **5**, 67-81.
Wisniewski, T., Ghiso, J. & Frangione, B. (1994). Alzheimer's disease and soluble Aβ. *Neurobiol. Aging*, **15**, 143-152.
Wood, S. J., Wetzel, R., Martin, J. D. & Hurle, M. R. (1995). Prolines and amyloidogenicity in fragments of the Alzheimer's peptide β/A4. *Biochemistry*, **34**, 724-730.
Wood, S. J., Chan, W. & Wetzel, R. (1996a). An apoE-Aβ inhibition complex in Aβ fibril extension. *Chem. Biol.* **3**, 949-956.
Wood, S. J., MacKenzie, L., Maleef, B., Hurle, M. R. & Wetzel, R. (1996b). Selective ihibition of Aβ fibril formation. *J. Biol. Chem.* **271(8)**, 4086-4092.
Wüthrich, K. (1986). *NMR of Proteins and Nucleic Acids*, Wiley, New York.
Yoshimoto, M., Iwai, A., Kang, D., Otero, D. A. C., Xia, Y. & Saitoh, T. (1995). NACP, the precursor protein of the non-amyloid β/A4 protein (Aβ) component of Alzheimer's disease amyloid, binds Aβ and stimulates Aβ aggregation. *Proc. Natl Acad. Sci. USA*, **92**, 9141-9145.
Younkin, S. G. (1995). Evidence that Aβ42 is the real culprit in Alzheimer's disease. *Ann. Neurol.* **37**, 287-288.
Zagorski, M. G. & Barrow, C. J. (1992). NMR studies of amyloid β-peptides: proton assignments, secondary structure, and mechanism of an α-helix → β-sheet conversion for a homologus, 28-residue, N-terminal fragment. *Biochemistry*, **31**, 5621-5631.
Zhang, H., Kaneko, K., Nguyen, J. T., Livshits, T. L., Baldwin, M. A., Cohen, F. E., James, T. & Prusiner, S. B. (1995). Conformational transitions in peptides containing two putative α-helices of the prion protein. *J. Mol. Biol.* **250**, 514-526.
Zhou, N. E., Zhu, B.-Y., Sykes, B. D. & Hodges, R. S. (1992). Relationship between amide proton chemical shifts and hydrogen bonding in amphipathic α-helical peptides. *J. Am. Chem. Soc.* **114**, 4320-3326.

Edited by P. E. Wright

(Received 5 June 1998; received in revised form 26 October 1998; accepted 26 October 1998)

http://www.academicpress.com/jmb

Supplementary Material comprising two Tables is available from JMB Online